



HAL
open science

Fluid phase equilibria prediction of fluorocompound-containing binary systems with the predictive E-PPR78 model

Jun-Wei Qian, Romain Privat, Jean-Noël Jaubert, Christophe Coquelet,
Deresh Ramjugernath

► **To cite this version:**

Jun-Wei Qian, Romain Privat, Jean-Noël Jaubert, Christophe Coquelet, Deresh Ramjugernath. Fluid phase equilibria prediction of fluorocompound-containing binary systems with the predictive E-PPR78 model . International Journal of Refrigeration, 2017, 73, pp.65-90. 10.1016/j.ijrefrig.2016.09.013 . hal-01387444

HAL Id: hal-01387444

<https://minesparis-psl.hal.science/hal-01387444>

Submitted on 25 Oct 2016

HAL is a multi-disciplinary open access archive for the deposit and dissemination of scientific research documents, whether they are published or not. The documents may come from teaching and research institutions in France or abroad, or from public or private research centers.

L'archive ouverte pluridisciplinaire **HAL**, est destinée au dépôt et à la diffusion de documents scientifiques de niveau recherche, publiés ou non, émanant des établissements d'enseignement et de recherche français ou étrangers, des laboratoires publics ou privés.

Fluid-phase-equilibrium prediction of fluorocompound-containing binary systems with the predictive *E*-PPR78 model

Jun-Wei QIAN^a, Romain PRIVAT^a, Jean-Noël JAUBERT^{a(*)},

Christophe COQUELET^{b,c} and Deresh RAMJUGERNATH^c

^a Université de Lorraine, Ecole Nationale Supérieure des Industries Chimiques, Laboratoire Réactions et Génie des Procédés (UMR CNRS 7274), 1 rue Grandville, 54000 Nancy, France.

^b Mines ParisTech, PSL Research University, CTP – Centre Thermodynamique des Procédés, 35 rue Saint Honoré, 77305 Fontainebleau Cedex, France.

^c Thermodynamics Research Unit, School of Engineering, University of KwaZulu-Natal, Howard College Campus, King George V Avenue, Durban 4041, South Africa.

E-mail: jean-noel.jaubert@univ-lorraine.fr - Fax number: +33 383175152 - Tel number: +33 383175081

(*) author to whom the correspondence should be addressed.

Abstract

In order to reduce the overall emissions of greenhouse gases and to be in compliance with the current environmental regulations, a new class of refrigerants, making use of fluorocompounds has appeared. Such refrigerants are often blends of alkanes, CO₂ and fluorocompounds. Consequently an equation of state (EoS) able to predict the properties of both pure compounds and multi-component systems is required to design processes involving fluorocompounds or to implement a product-design approach aimed at identifying new refrigerant mixtures. It is however well-acknowledged that the phase behavior of binary systems like, e.g., an alkane and its corresponding perfluoroalkane, show significant deviations from ideality that need to be accurately accounted for by a thermodynamic model. In this study, in order to get a predictive model applicable to fluorocompound-containing binary systems, six groups were added to the Enhanced-PPR78 model which combines the Peng-Robinson EoS and a group contribution method aimed at estimating the binary interaction parameters, $k_{ij}(T)$, involved in Van der Waals one-fluid mixing rules.

Keywords: equation of state, PPR78, vapor-liquid equilibrium, predictive model, binary interaction parameters, fluorocompound, critical locus, azeotropy.

1. INTRODUCTION

Fluorocompounds have gained recently a noticeable interest in industry because of their remarkable properties for a wide range of applications, including the development of alternative environmentally-friendly refrigerants, fire-extinguishers, foam blowing agents, lubricants and specific solvents. For each of these applications and some others, it is desirable to be able to benchmark a large number of fluorocompound-containing mixtures through a so-called *product-design approach* in order to find out the most appropriate one. In particular, it is absolutely necessary to be able to predict the fluid-phase behavior of such mixtures in both the sub- and super-critical regions.

A literature review highlighted that vapor-liquid equilibrium (VLE) and liquid-liquid equilibrium (LLE) data of fluorocompound-containing systems could be efficiently correlated by cubic equations of state (EoS). As a first example, Coquelet et al. [1] were able to accurately correlate the phase behavior of the azeotropic [R32(1) + propane(2)] system by combining the Soave-Redlich-Kwong (SRK) EoS and the NRTL model through advanced mixing rules. A few years later, Subramoney et al. [2] regressed the experimental VLE data of refrigerant-containing systems to parameterize three different thermodynamic packages: the Peng-Robinson (PR) EoS with the Wong-Sandler (WS) mixing rules, the PR EoS with the modified Huron-Vidal first-order (MHV1) mixing rules, and the SRK EoS with the WS mixing rules. The Mathias-Copeman alpha function was selected and the non-random two-liquid (NRTL) excess Gibbs energy model was incorporated to the mixing rules. They concluded that the best correlation of the experimental data is obtained by using the PR EoS combined with the WS mixing rules. The same conclusion was drawn by El Ahmar et al. [3] working on the modelling of VLE and critical data of the [ethane(1) + perfluorobutane(2)] system. Some other authors also demonstrated that the experimental VLE data of several refrigerant-containing systems [4-8] could be correlated with the PR EoS coupled with the NRTL model through the WS mixing rules.

It is well known that n-alkanes and perfluoroalkane are both non-polar species. Consequently, it is expected that systems containing an alkane and its corresponding perfluoroalkane mix almost ideally. As a counterintuitive result, they display actually significant positive deviations from ideality, showing extensive regions of liquid-liquid immiscibility associated with an upper critical solution temperature (UCST). To model such systems, statistical associating fluid theory (SAFT) -based EoS were investigated by numerous researchers. By applying the SAFT-VR approach, Morgado et al. [9] were able to

model the phase and volumetric behavior of the (n-alkane + perfluoroalkane) binary mixtures. Their EoS was parameterized by simultaneously fitting the UCST and excess-molar-volume data of the sole n-hexane + perfluorohexane system. They concluded that the SAFT-VR model was able to accurately predict the VLE, LLE and excess-molar-volume data of these systems. Pratas de Melo et al. [10] used the soft-SAFT EoS with parameters fitted on VLE data of perfluorooctane + alkane binary mixtures and demonstrated their transferability to the LLE data they measured, thus pointing out the predictive capacity of the soft-SAFT model. Aparicio [11] carried out a study on the phase-equilibrium behavior of perfluoroalkane + alkane binary mixtures using the PC-SAFT EoS coupled to the Lorentz-Berthelot mixing rule involving adjustable and temperature-independent binary interaction parameters. The general shape of the *global phase-equilibrium diagrams* (GPED) [12-13] of these mixtures could be qualitatively but not quantitatively predicted by the PC-SAFT model. Moreover, SAFT models often fail to predict the phase behavior in the critical region, which is a great disadvantage in comparison with cubic EoS. Recently, Lafitte et al. [14] proposed a new SAFT EoS (SAFT VR Mie) characterized by the use of the Mie potential to describe the attractive and repulsive interactions between the segments which build the molecules. This equation of state leads to better prediction of the critical region but in return more parameters have to be fitted on experimental data.

Our literature review makes it possible to conclude that phase-equilibrium prediction for fluorocompound-containing binary mixtures in a wide range of temperatures and pressures is still a challenge. It is worth noting that for such systems, it is not possible to use the so-called γ - ϕ approach which combines an equation of state to model the gas phase and an activity-coefficient model (like UNIFAC) to represent the liquid phase since such an approach is not adapted to perform calculations in the supercritical region.

In the last ten years, the PPR78 (Predictive 1978, Peng-Robinson equation of state) model, which was originally proposed by Jaubert and co-workers [15], has been shown to be accurate and reliable for the prediction of the phase-equilibrium behavior of mixtures containing hydrocarbons [15-18], permanent gases [19-25], sulfur compounds [26-28], water [29], esters [30-32] and even some refrigerants like the R1234yf and the R1234ze [33]. The PPR78 model has been also successfully applied to phase-envelope prediction of petroleum fluids [34-36]. Recently, Qian et al. [37] published predictions of enthalpy and heat-capacity changes on mixing with the PPR78 model. They concluded that predictions of property changes on mixing could be highly improved by simultaneously fitting the group-interaction parameters on vapor-liquid equilibrium, enthalpy and heat-capacity change-on-mixing data. Such a work

was performed by Qian during his thesis [38] and the resulting model was called *E*-PPR78 (Enhanced Predictive Peng-Robinson, 1978). This model, which combines the widely used PR EoS with a group-contribution method aimed at estimating the temperature-dependent binary interaction parameters $k_{ij}(T)$, can also be seen as the combination of the PR EoS with a 1-parameter Van Laar type activity-coefficient (g^E) model under infinite pressure [39] through the well-established Huron-Vidal mixing rules. Consequently, expected to be a good candidate for the design of new refrigerants, the *E*-PPR78 model was extended to fluorocompounds through the addition of six new structural groups: C_2F_6 (single molecule named R116, according to the ASHRAE classification), $-CF_3$, $-CF_2-$, $=CF_2 \leftrightarrow =CF$, $C_2H_4F_2$ (single molecule R152a) and $C_2H_2F_4$ (single molecule R134a). It is worth recalling that group-contribution methods fail to describe the first members of a homologous series explaining why it is neither recommended to divide ethane in two CH_3 groups nor R116 in two CF_3 groups. Similarly, it is not advised to divide R152a and R134a which only contain 2 carbon atoms in two groups: it is preferred to view each of these 2 molecules as a single group in order not to lose accuracy.

In the framework of the present study, the interactions between these six new groups and the groups previously defined were determined. It is thus today possible to predict, at any temperature, the k_{ij} coefficient between two components in any mixture containing paraffins, aromatics, naphthenes, CO_2 , N_2 , H_2S , mercaptan, H_2 , olefins, water and fluorocompounds (only refrigerants with more than 2 carbon atoms can be modeled).

2. THE E-PPR78 MODEL

In 1978, Peng and Robinson published an improved version of their well-known equation of state, referred to as PR78 in this paper [40]. For a pure component, the PR78 EoS is:

$$P = \frac{RT}{v - b_i} - \frac{a_i(T)}{v(v + b_i) + b_i(v - b_i)} \quad (1)$$

and:

$$\left\{ \begin{array}{l} R = 8.314472 \text{ J} \cdot \text{mol}^{-1} \cdot \text{K}^{-1} \\ \eta_c = \left[1 + \sqrt[3]{4 - 2\sqrt{2}} + \sqrt[3]{4 + 2\sqrt{2}} \right]^{-1} \approx 0.253076587 \\ b_i = \Omega_b \frac{RT_{c,i}}{P_{c,i}} \text{ with: } \Omega_b = \frac{\eta_c}{\eta_c + 3} \approx 0.0777960739 \\ a_i = \Omega_a \frac{R^2 T_{c,i}^2}{P_{c,i}} \alpha(T) \text{ with: } \Omega_a = \frac{40\eta_c + 8}{49 - 37\eta_c} \approx 0.457235529 \text{ and } \alpha(T) = \left[1 + m_i \left(1 - \sqrt{\frac{T}{T_{c,i}}} \right) \right]^2 \\ \text{if } \omega_i \leq 0.491 \quad m_i = 0.37464 + 1.54226\omega_i - 0.26992\omega_i^2 \\ \text{if } \omega_i > 0.491 \quad m_i = 0.379642 + 1.48503\omega_i - 0.164423\omega_i^2 + 0.016666\omega_i^3 \end{array} \right. \quad (2)$$

where P is the pressure, R is the gas constant, T is the temperature, a_i and b_i are the cohesive parameter and molar covolume of pure component i , v is the molar volume, $T_{c,i}$ is the experimental critical temperature, $P_{c,i}$ is the experimental critical pressure and ω_i is the experimental acentric factor of pure i . To apply this EoS to a mixture, mixing rules are necessary to calculate the values of a and b of the mixture. Classical Van der Waals one-fluid mixing rules are used in the E-PPR78 model:

$$\left\{ \begin{array}{l} a(T, \mathbf{z}) = \sum_{i=1}^N \sum_{j=1}^N z_i z_j \sqrt{a_i(T) \cdot a_j(T)} [1 - k_{ij}(T)] \\ b(\mathbf{z}) = \sum_{i=1}^N z_i b_i \end{array} \right. \quad (3)$$

where z_i represents the mole fraction of component i and N is the number of components in the mixture. The $k_{ij}(T)$ parameter, whose estimation is difficult even for the simplest systems, is the so-called binary interaction parameter (BIP) characterizing the molecular interactions between molecules i and j . Although the common practice is to fit k_{ij} to reproduce the vapor-liquid equilibrium data of the mixture under consideration, the predictive PPR78 model calculates the k_{ij} value, which is temperature-dependent, with a group contribution method

using the following expression [15]:

$$k_{ij}(T) = \frac{-\frac{1}{2} \left[\sum_{k=1}^{N_g} \sum_{l=1}^{N_g} (\alpha_{ik} - \alpha_{jk})(\alpha_{il} - \alpha_{jl}) A_{kl} \cdot \left(\frac{298.15}{T/K} \right)^{\left(\frac{B_{kl}-1}{A_{kl}} \right)} \right] - \left(\frac{\sqrt{a_i(T)}}{b_i} - \frac{\sqrt{a_j(T)}}{b_j} \right)^2}{2 \frac{\sqrt{a_i(T) \cdot a_j(T)}}{b_i \cdot b_j}} \quad (4)$$

In Eq. (4), T is the temperature. The a_i and b_i values are given in Eq. (2). The N_g variable is the number of different groups defined by the group-contribution method (for the time being, twenty seven groups are defined, and $N_g = 27$). The α_{ik} variable is the fraction of molecule i occupied by group k (occurrence of group k in molecule i divided by the total number of groups present in molecule i). The group-interaction parameters, $A_{kl} = A_{lk}$ and $B_{kl} = B_{lk}$ (where k and l are two different groups), were determined in our previous papers [15-29]. To extend the E -PPR78 model to the class of fluorocompounds, it is necessary to estimate the group-interaction parameters between the six new groups added in this paper [group 22 = C_2F_6 (R116), group 23 = CF_3 , group 24 = CF_2 , group 25 = $CF_{2, \text{double bond}} \leftrightarrow CF_{\text{double bond}}$, group 26 = $C_2H_4F_2$ (R152a), group 27 = $C_2H_2F_4$ (R134a)] and the twenty-one others previously defined. We thus need to estimate 282 parameters (141 A_{kl} and 141 B_{kl} values). However, due to a lack of experimental data, it was only possible to get the values of 110 new parameters (55 A_{kl} and 55 B_{kl} values). These parameters were determined in order to minimize the deviations between calculated and experimental data from an extended database. The corresponding A_{kl} and B_{kl} values (expressed in MPa) are summarized in Table 1.

3. DATABASE AND REDUCTION PROCEDURE

Table 2 lists the 35 pure components involved in this study. The pure-fluid physical properties ($T_{c,i}$, $P_{c,i}$ and ω_i) that were used in this study originate from two sources. Poling et al. [41] was used for alkanes, cyclo-alkanes, aromatic compounds, CO₂, alkenes. The DIPPR database was used for the fluorocompounds since they were not all available in [41]. As a noticeable exception, the properties of pure hexafluoropropylene were extracted from Coquelet et al. [95] since such authors clearly demonstrated that the values reported in the DIPPR database were wrong. Table 3 details the sources of the binary experimental data used in our evaluations [2-8, 42-94] along with the temperature, pressure and composition range for each binary system. Additionally, some experimental data for the four following binary systems:

1. hexafluoroethane(1) + n-butane(2),
2. hexafluoroethane(1) + n-pentane(2),
3. hexafluoroethane(1) + n-hexane(2),
4. ethane(1) + hexafluoroethane(2),

are not yet published. They were acquired by Professors Coquelet and Ramjugernath from MINES ParisTech and Kwazulu Natal University respectively. Such measurements were conducted in 2007 during the one stay in France of Pr. D. Ramjugernath using an equipment lying on the static analytic method [96]. The data measured in the context of this scientific exchange were used in the data regression procedure.

Most of the data available in the open literature (2214 bubble points + 1938 dew points + 93 mixture critical points) were collected. Our database includes VLE data on 64 binary systems. The 104 parameters (52 A_{kl} and 52 B_{kl}) determined in this study (see Table 1), were obtained by minimizing the following objective function:

$$F_{\text{obj}} = \frac{F_{\text{obj, bubble}} + F_{\text{obj, dew}} + F_{\text{obj, crit.comp}} + F_{\text{obj, crit.pressure}}}{n_{\text{bubble}} + n_{\text{dew}} + 2n_{\text{crit}}} \quad (5)$$

$$\left\{ \begin{array}{l} F_{\text{obj, bubble}} = 100 \sum_{i=1}^{n_{\text{bubble}}} 0.5 \left(\frac{|\Delta x|}{x_{1, \text{exp}}} + \frac{|\Delta x|}{x_{2, \text{exp}}} \right)_i \quad \text{with } |\Delta x| = |x_{1, \text{exp}} - x_{1, \text{cal}}| = |x_{2, \text{exp}} - x_{2, \text{cal}}| \\ F_{\text{obj, dew}} = 100 \sum_{i=1}^{n_{\text{dew}}} 0.5 \left(\frac{|\Delta y|}{y_{1, \text{exp}}} + \frac{|\Delta y|}{y_{2, \text{exp}}} \right)_i \quad \text{with } |\Delta y| = |y_{1, \text{exp}} - y_{1, \text{cal}}| = |y_{2, \text{exp}} - y_{2, \text{cal}}| \\ F_{\text{obj, crit, comp}} = 100 \sum_{i=1}^{n_{\text{crit}}} 0.5 \left(\frac{|\Delta x_c|}{x_{c1, \text{exp}}} + \frac{|\Delta x_c|}{x_{c2, \text{exp}}} \right)_i \quad \text{with } |\Delta x_c| = |x_{c1, \text{exp}} - x_{c1, \text{cal}}| = |x_{c2, \text{exp}} - x_{c2, \text{cal}}| \\ F_{\text{obj, crit, pressure}} = 100 \sum_{i=1}^{n_{\text{crit}}} \left(\frac{|P_{\text{cm, exp}} - P_{\text{cm, cal}}|}{P_{\text{cm, exp}}} \right)_i \end{array} \right.$$

where n_{bubble} , n_{dew} , and n_{crit} , are the number of bubble points, dew points and mixture critical points, respectively. The variable, x_1 , is the mole fraction of the most volatile component in the liquid phase, and x_2 is the mole fraction of the heaviest component ($x_2 = 1 - x_1$) at a fixed temperature and pressure. Similarly, y_1 is the mole fraction of the most volatile component in the gas phase, and y_2 is the mole fraction of the heaviest component ($y_2 = 1 - y_1$) at a fixed temperature and pressure. The variable x_{c1} is the critical mole fraction of the most volatile component, and x_{c2} is the critical mole fraction of the heaviest component at a fixed temperature. P_{cm} is the binary critical pressure at a fixed temperature.

4. ON THE DIFFICULT SIMULTANEOUS PREDICTION OF THE LIQUID-LIQUID MISCIBILITY GAP AND VALUE OF THE UPPER CRITICAL SOLUTION TEMPERATURE (UCST)

A n-alkane and its corresponding perfluoroalkane exhibit similar structures since in a perfluoroalkane, the hydrogen atoms in the n-alkane molecule are simply replaced by fluorine atoms. Hence, the perfluoroalkane and its corresponding alkane could be expected to mix almost ideally. However, it is noticed that the two kinds of pure components are very different in terms of physico-chemical properties and the corresponding binary systems show actually significant deviations to ideality. As an example, let us consider the system perfluoro-n-pentane(1) + n-pentane(2). Vapor-liquid equilibria (VLE) of this system at high pressures, including the critical region, were investigated by Aftienjew and Zawisza [42]. As shown in Fig. 1a and 1b, not only the *global phase equilibrium diagram* (GPED) [12] but also the location of the azeotropes are in good agreement with experimental data points demonstrating that the *E-PPR78* model is capable to accurately reproduce VLE data at temperatures higher than that of the UCST as well as type II phase behavior (note that *Type II* refers to the classification scheme of Van Konynenburg and Scott [12,97]).

Additionally, this system was also examined by Simons and Dunlap [82] who measured the complete liquid-liquid phase diagram (see Fig. 1c, 1d and 1e). As highlighted in Fig. 1c, such a system exhibits a large liquid-liquid immiscibility gap that persists up to 265.5 K (measured UCST). The parameters A_{kl} and B_{kl} of the *E-PPR78* model were estimated by considering experimental VLE data only. It is thus not surprising to observe a poor description of the LLE phase diagram (see Fig. 1c). Moreover, the predicted UCST is about 28 K higher than the experimental one (see Fig. 1c and 1d). As a consequence, at temperatures ranging between the experimental and predicted UCST, the *E-PPR78* model predicts heteroazeotropy whereas experimental measurements indicate homoazeotropy (see, e.g., isothermal phase diagrams at 278.60 K, 283.10 K and 288.20 K in Fig. 1e). In spite of this limitation, most of the experimental bubble and dew points are accurately predicted by the *E-PPR78* model. More generally, the limitations and successes described in this section also apply to the other binary mixtures alkane + perfluoroalkane involved in the present study.

5. RESULTS AND DISCUSSION

For all the data points included in our database, the objective function defined by Eq. (5) is:

$$F_{\text{obj}} = 9.41\%.$$

The average overall deviation on the liquid-phase composition is:

$$\overline{\Delta x_1} = \frac{\sum_{i=1}^{n_{\text{bubble}}} (|x_{1,\text{exp}} - x_{1,\text{cal}}|)_i}{n_{\text{bubble}}} = 0.034. \text{ Moreover } \frac{F_{\text{obj,bubble}}}{n_{\text{bubble}}} = 11.66\%$$

The average overall deviation on the gas-phase composition is:

$$\overline{\Delta y_1} = \frac{\sum_{i=1}^{n_{\text{dew}}} (|y_{1,\text{exp}} - y_{1,\text{cal}}|)_i}{n_{\text{dew}}} = 0.023. \text{ Moreover } \frac{F_{\text{obj,dew}}}{n_{\text{dew}}} = 6.84\%$$

The average overall deviation on the critical composition is:

$$\overline{\Delta x_{c1}} = \frac{\sum_{i=1}^{n_{\text{crit}}} (|x_{c1,\text{exp}} - x_{c1,\text{cal}}|)_i}{n_{\text{crit}}} = 0.047. \text{ Moreover } \frac{F_{\text{obj,crit. comp}}}{n_{\text{crit}}} = 16.64\%$$

The average overall deviation on the binary critical pressure is:

$$\overline{\Delta P_c} \% = \frac{F_{\text{obj,crit. pressure}}}{n_{\text{crit}}} = \frac{100 \sum_{i=1}^{n_{\text{crit}}} \left(\frac{|P_{\text{cm,exp}} - P_{\text{cm,cal}}|}{P_{\text{cm,exp}}} \right)_i}{n_{\text{crit}}} = 2.93\%$$

Although higher than the ones obtained with hydrocarbon-hydrocarbon systems [15-17], the values of the objective function and related overall deviations indicate that the *E*-PPR78 model can be safely used to predict the phase behavior of systems involving fluorocompounds.

The following reasons can be invoked to explain a posteriori the objective-function value:

(1) Phase diagrams exhibiting homoazeotropy are frequently encountered in this study and as explained in several of our previously-published papers [26,27], such a behavior tends to make increase the objective function.

(2) The PR78 EoS is not able to predict the vapor pressure of several pure components with sufficient accuracy. Consequently, the very narrow phase diagrams, experimentally observed for mixtures containing 2 fluorocompound isomers (see e.g., the 1,1,1,2-tetrafluoroethane + 1,1-difluoroethane system) are not accurately predicted; similar issues were previously encountered in our study dealing with alkene-containing mixtures [18].

(3) As discussed in the previous section, experimentally-observed homoazeotropy is likely to be predicted as heteroazeotropy by the *E*-PPR78 model which generates unrealistic liquid-liquid equilibria; as a consequence, significant deviations on the liquid phase composition are observed in the vicinity of unrealistic 3-phase (vapor-liquid-liquid) lines explaining why absolute deviation and percent deviation on the liquid phase composition are much higher than for gas phase.

In order to illustrate the accuracy and the limitations of the *E*-PPR78 model, it was decided to define several families of binary systems in order to give a fair overview of the whole database.

5.1 Results for mixtures containing a fluorocompound + a n-alkane

In this family, 954 bubble points, 841 dew points and 74 critical points were collected for 29 binary mixtures. Although our database includes 14 different fluorocompounds, no phase-equilibrium data for binary mixtures containing methane was found in the open literature. Consequently, it was not possible to determine the 12 group-interaction parameters (6 A_{kl} and 6 B_{kl}) between the six new groups defined in this study and group CH₄ (methane). Moreover, we did not find data for systems including a n-alkane heavier than the n-nonane. In [Figs. 2-5](#), most of the phase diagrams predicted by the *E*-PPR78 model, together with experimental points, are represented.

[Fig. 2](#) shows isothermal phase diagrams, ranging from the subcritical to the critical region, for three binary systems ethane + fluorocompound. It is noticeable that the phase behavior of the ethane(1) + hexafluoroethane(2) system (see [Fig. 2a](#) and [2b](#)) is very similar to the one of the CO₂(1) + ethane(2) system [\[21\]](#). In particular, such a system exhibits absolute azeotropy and the isothermal phase diagram plotted at 288.25 K displays two vapor-liquid critical points. This last feature is the consequence of a temperature minimum on the critical locus connecting the vapor-liquid critical points of the two pure components [\[98,99\]](#). For such systems, very accurate results are obtained and the k_{ij} varies from 0.1266 to 0.1341 as the temperature increases from 189.31 K to 296.23 K. A similar accuracy is observed with the other two ethane-containing binary systems (see [Fig. 2c](#) and [2d](#)).

[Fig. 3](#) shows the isothermal phase diagrams of four binary systems consisting of propane and a fluorocompound. [Fig. 3a](#), [3b](#) and [3c](#) highlight that positive azeotropy in the subcritical region is well described by the model although the azeotropic pressure of the propane(1) +

perfluoro-n-butane(2) system at 342.94 K is slightly overestimated. The predicted isothermal phase diagrams of the hexafluoroethane(1) + propane(2) system, both in the subcritical and critical regions, are in good agreement with experimental VLE data.

Fig. 4 shows various isothermal P_{xy} phase diagrams for five binary systems consisting of a fluorocompound and a n-alkane (n-butane, n-pentane and n-hexane). A general overview of the results obtained indicates that our model is able to perfectly capture these data. Note that the hexafluoroethane(1) + n-hexane(2) system at 288.24 K exhibits a VLL 3-phase line which is experimentally confirmed (Fig. 4e).

Fig. 5 shows the P_{xy} diagrams for four binary systems containing a n-alkane and the corresponding perfluoro-n-alkane. As previously discussed in the case of the perfluoro-n-pentane(1) + n-pentane(2) system, the E -PPR78 model cannot capture perfectly the experimental upper critical solution temperature (UCST) and the predicted value is always higher than the experimental one. Consequently, heteroazeotropy is predicted instead of the experimentally-observed homoazeotropy at temperatures ranging between the experimental and calculated UCST (see Fig. 5a, 5b, 5c and 5d). Despite this limitation, calculated VLE curves are in close agreement with experimental data. Note that one isotherm of the system propane(1) + perfluoropropane(2) in Fig. 5a and two isotherms of the system perfluoro-n-butane(1) + n-butane(2) in Fig. 5b are located at temperatures higher than predicted UCST and experimental homoazeotropy is perfectly reproduced.

Fig. 5e and 5f show the critical loci for thirteen binary mixtures consisting of a fluorocompound and a n-alkane. All these systems exhibit a continuous vapor–liquid critical curve between the critical points of two pure components; such a behavior indicates a type I or II according to the classification scheme of Van Konynenburg and Scott [12,97]. Generally, all the critical loci are satisfactorily predicted in a qualitative and quantitative ways by the model despite the slight overestimation (see Fig. 5f) of the pressure-maximum for the systems perfluoro-n-heptane(1) + n-octane(2) and perfluoro-n-heptane(1) + n-nonane(2).

5.2 Results for mixtures containing a fluorocompound + a branched alkane

200 bubble-point, 180 dew-point and 0 critical-point data were reported for six binary mixtures containing a fluorocompound + a branched alkane. Fig. 6 shows the isothermal phase diagrams for four of these binary systems. The locus of positive homoazeotropes predicted by the E -PPR78 model is in close agreement with experimental data. As previous, the heteroazeotropy phenomenon is predicted instead of the experimentally-observed homoazeotropy for the system perfluoro-n-heptane(1) + 3-methylheptane(2) at four different

temperatures (see Fig. 6c) and for the system perfluoro-n-heptane(1) + 2,2,4-trimethylpentane at one temperature (see Fig. 6d). Since no experimental critical point was available for parameter estimation, note that predictions of VLE in the critical region should be considered with caution.

5.3 Results for mixtures containing a fluorocompound + an aromatic or a naphthenic compound

In this family, while 30 pairs of group-interaction parameters (A_{kl} and B_{kl}) should have been estimated, only 8 pairs were finally determined (see Table 1) due to a lack of data for binary mixtures containing a fluorocompound and an aromatic or a naphthenic compound. Only 107 bubble points, 85 dew points and 0 critical point for 7 binary mixtures were reported in our database.

Fig. 7 shows the isothermal phase diagrams for four different binary systems. All the available experimental data, including both symmetric (see Fig. 7a, 7b and 7c) and size-asymmetric mixtures (see Fig. 7d) are accurately predicted. Once again, no experimental critical point was available so that it is impossible to guarantee proper phase-equilibrium predictions in the critical region.

5.4 Results for mixtures containing a fluorocompound + CO₂

According to our database, 398 bubble-point data, 278 dew-point data and 15 mixture critical-point data were collected for 8 binary mixtures containing a fluorocompound + CO₂, making possible the estimation of 12 group-interaction parameters (6 A_{kl} and 6 B_{kl} values). Figs. 8-9 not only show the isothermal phase diagrams predicted by the *E*-PPR78 model for seven systems consisting of CO₂ and a fluorocompound but also show the critical loci for 4 binary systems.

Having a look at all these graphical results and having in mind that the objective-function value is as low as 4 % for all the experimental data points belonging to this class of binary systems, makes it possible to conclude that *E*-PPR78 is capable of accurately predicting the phase behavior of such systems. Figs. 8c, 9c, 9d and 9e however highlight that in spite of an accurate prediction of the critical composition, *E*-PPR78 tends to underestimate the critical pressures.

5.5 Results for mixtures containing a fluorocompound + an alkene

In this study, 372 bubble points, 368 dew points and 4 critical points were collected for 8 binary mixtures containing a fluorocompound + an alkene. While 24 pairs of parameters (A_{kl} and B_{kl}) should have been estimated, only 9 pairs were finally determined (see [Table 1](#)). [Fig. 10](#) shows the phase diagrams predicted by the *E*-PPR78 model for six systems consisting of an alkene and a fluorocompound. Experimental VLE data are predicted with an excellent accuracy, including the critical region for the system ethylene(1) + hexafluoropropylene(2) (see [Fig. 10a](#)) and the positive homoazeotropy exhibited by the five other binary mixtures ([Fig. 10b](#), [10c](#), [10d](#), [10e](#) and [10f](#)). The 4 experimentally-determined critical points of the ethylene(1) + 3,3,3-trifluoro-1-propene(2) system are visible on the GPED reported in [Fig. 9e](#). Although reasonable deviations are observed for these 4 critical pressures, the lack of sufficient amount of critical information makes us believe that one should take care when using the model to predict VLE in the critical region.

5.6 Results for mixtures containing two fluorocompounds

In this family, 183 bubble points, 186 dew points and no critical points were collected for 6 binary mixtures. [Fig. 11](#) shows the isothermal and isobaric phase diagrams for five binary systems consisting of two fluorocompounds. A general overview of the obtained graphical results makes it possible to conclude that most of the experimental data points are predicted accurately except the UCST of the perfluoropropane(1) + 1,1-difluoroethane(2) which is overestimated (see [Fig. 11e](#) and [11f](#)). As previously discussed, the reproduction of such a temperature by the *E*-PPR78 model is difficult. Once again, no experimental critical points were used for parameter estimation in this family, so that predictions of VLE in the critical region should be considered with caution.

6. CONCLUSION

In this work, the *E*-PPR78 model was extended to fluorocompound-containing systems. While 141 pairs of group-interaction parameters (A_{kl} and B_{kl}) should have been determined, only 55 pairs were estimated because of a lack of experimental information. Consequently, the present model is today unable to predict phase equilibria in mixtures containing a fluorocompound and either methane, nitrogen, H₂S, a mercaptan, H₂O or H₂.

Table 3 highlights that critical loci were only measured for a restricted number of binary systems. As a result, the influence of such points on the group-interaction parameter fitting is weak and it is not possible to ensure accurate predictions of phase-equilibrium properties in the critical region.

This study also makes it possible to conclude that for systems composed of a n-alkane and its corresponding perfluoro-n-alkane, the *E*-PPR78 model always overestimates the experimentally-observed upper critical solution temperature (UCST) which is the above-limit of the liquid-liquid region. This behavior entails the prediction of heteroazeotropes instead of the experimentally-observed homoazeotropes. In spite of this limitation, predictions of bubble and dew curves are in excellent agreement with experimental data.

Generally speaking, the combination of satisfactory graphical results and reasonable deviations (in particular, the objective function defined in Eq. (5) is lower than 10 %) clearly indicates that the proposed model can be safely used to design processes involving fluorocompounds or to implement a product-design approach aimed at identifying new refrigerant mixtures. This paper also makes it possible to conclude that more experimental data, especially VLE, VLLE and mixture critical points are needed to improve the current accuracy of predictive thermodynamic models.

LIST OF SYMBOLS

$a(T)$ = temperature-dependent cohesive parameter of the PR equation of state [$\text{Pa} \cdot \text{m}^6 \cdot \text{mol}^{-2}$]

A_{kl}, B_{kl} = constant group-interaction parameters [Pa]

b = molar covolume [$\text{m}^3 \cdot \text{mol}^{-1}$]

k_{ij} = binary interaction parameter

m = shape parameter

P = pressure [Pa]

P_c = critical pressure [Pa]

PR = Peng-Robinson

R = gas constant [$\text{J} \cdot \text{mol}^{-1} \cdot \text{K}^{-1}$]

T = temperature [K]

T_c = critical temperature [K]

v = molar volume [$\text{m}^3 \cdot \text{mol}^{-1}$]

VLE = Vapor-liquid equilibrium

x_i, y_i, z_i = mole fractions of component i (x is used in a liquid phase, y , in a gas phase and z when the aggregation state is not known)

Greek letters:

ω = acentric factor

α_{ik} = fraction occupied by group k in the molecule i

ACKNOWLEDGMENT

The French Petroleum Company TOTAL and more particularly Dr. Pierre DUCHET–SUCHAUX and Dr. Laurent AVAULLÉE (experts in thermodynamics) are gratefully acknowledged for sponsoring this research.

Table 1. Group-interaction parameters: ($A_{kl} = A_{lk}$)/MPa and ($B_{kl} = B_{lk}$)/MPa. Only the parameters in the last six lines of this tables, relative to the fluorocompound groups were determined in this work. The other parameters were determined by Qian [38].

	CH ₃ (group 1)	CH ₂ (group 2)	CH (group 3)	C (group 4)	CH ₄ (group 5)	C ₂ H ₆ (group 6)	CH _{aro} (group 7)	C _{aro} (group 8)	C _{fused aromatic rings} (group 9)	CH _{2,cyclic} (group 10)	CH _{cyclic} /C _{cyclic} (group 11)	CO ₂ (group 12)	N ₂ (group 13)
CH ₃ (group 1)	0	-	-	-	-	-	-	-	-	-	-	-	
CH ₂ (group 2)	A ₁₂ = 65.54 B ₁₂ = 105.7	0	-	-	-	-	-	-	-	-	-	-	
CH (group 3)	A ₁₃ = 214.9 B ₁₃ = 294.9	A ₂₃ = 39.05 B ₂₃ = 41.59	0	-	-	-	-	-	-	-	-	-	
C (group 4)	A ₁₄ = 431.6 B ₁₄ = 575.0	A ₂₄ = 134.5 B ₂₄ = 183.9	A ₃₄ = -86.13 B ₃₄ = 85.10	0	-	-	-	-	-	-	-	-	
CH ₄ (group 5)	A ₁₅ = 28.48 B ₁₅ = 20.25	A ₂₅ = 37.75 B ₂₅ = 74.81	A ₃₅ = 131.4 B ₃₅ = 157.5	A ₄₅ = 309.5 B ₄₅ = 35.69	0	-	-	-	-	-	-	-	
C ₂ H ₆ (group 6)	A ₁₆ = 3.775 B ₁₆ = 8.922	A ₂₆ = 29.85 B ₂₆ = 65.88	A ₃₆ = 156.1 B ₃₆ = 96.77	A ₄₆ = 388.1 B ₄₆ = -224.8	A ₅₆ = 9.951 B ₅₆ = 13.73	0	-	-	-	-	-	-	
CH _{aro} (group 7)	A ₁₇ = 98.83 B ₁₇ = 136.2	A ₂₇ = 25.05 B ₂₇ = 64.51	A ₃₇ = 56.62 B ₃₇ = 129.7	A ₄₇ = 170.5 B ₄₇ = 284.1	A ₅₇ = 67.26 B ₅₇ = 167.5	A ₆₇ = 41.18 B ₆₇ = 50.79	0	-	-	-	-	-	
C _{aro} (group 8)	A ₁₈ = 103.60 B ₁₈ = 103.60	A ₂₈ = 5.147 B ₂₈ = -7.549	A ₃₈ = 48.73 B ₃₈ = -89.22	A ₄₈ = 128.3 B ₄₈ = 189.1	A ₅₈ = 106.7 B ₅₈ = 190.8	A ₆₈ = 67.94 B ₆₈ = 210.7	A ₇₈ = -16.47 B ₇₈ = 16.47	0	-	-	-	-	
C _{fused aromatic rings} (group 9)	A ₁₉ = 624.9 B ₁₉ = 774.10	A ₂₉ = -17.84 B ₂₉ = -4.118	NA	NA	A ₅₉ = 249.1 B ₅₉ = 408.3	NA	A ₇₉ = 52.50 B ₇₉ = 251.2	A ₈₉ = -328.0 B ₈₉ = -569.3	0	-	-	-	
CH _{2,cyclic} (group 10)	A ₁₋₁₀ = 43.58 B ₁₋₁₀ = 60.05	A ₂₋₁₀ = 8.579 B ₂₋₁₀ = 27.79	A ₃₋₁₀ = 73.09 B ₃₋₁₀ = 71.37	A ₄₋₁₀ = 208.6 B ₄₋₁₀ = 294.4	A ₅₋₁₀ = 33.97 B ₅₋₁₀ = 5.490	A ₆₋₁₀ = 12.70 B ₆₋₁₀ = 73.43	A ₇₋₁₀ = 28.82 B ₇₋₁₀ = 65.54	A ₈₋₁₀ = 37.40 B ₈₋₁₀ = 53.53	A ₉₋₁₀ = 140.7 B ₉₋₁₀ = 277.6	0	-	-	
CH _{cyclic} /C _{cyclic} (group 11)	A ₁₋₁₁ = 293.4 B ₁₋₁₁ = 170.9	A ₂₋₁₁ = 63.48 B ₂₋₁₁ = -74.46	A ₃₋₁₁ = -120.8 B ₃₋₁₁ = 18.53	A ₄₋₁₁ = 25.05 B ₄₋₁₁ = 81.33	A ₅₋₁₁ = 188.0 B ₅₋₁₁ = 473.9	A ₆₋₁₁ = 118.0 B ₆₋₁₁ = -212.8	A ₇₋₁₁ = 129.0 B ₇₋₁₁ = 36.72	A ₈₋₁₁ = -99.17 B ₈₋₁₁ = -193.5	A ₉₋₁₁ = -99.17 B ₉₋₁₁ = -193.5	A ₁₀₋₁₁ = 139.0 B ₁₀₋₁₁ = 35.69	0	-	
CO ₂ (group 12)	A ₁₋₁₂ = 144.8 B ₁₋₁₂ = 401.5	A ₂₋₁₂ = 141.4 B ₂₋₁₂ = 237.1	A ₃₋₁₂ = 191.8 B ₃₋₁₂ = 380.9	A ₄₋₁₂ = 377.5 B ₄₋₁₂ = 162.7	A ₅₋₁₂ = 134.9 B ₅₋₁₂ = 219.3	A ₆₋₁₂ = 136.2 B ₆₋₁₂ = 235.7	A ₇₋₁₂ = 98.48 B ₇₋₁₂ = 253.6	A ₈₋₁₂ = 154.4 B ₈₋₁₂ = 374.4	A ₉₋₁₂ = 331.1 B ₉₋₁₂ = 276.6	A ₁₀₋₁₂ = 144.1 B ₁₀₋₁₂ = 354.1	A ₁₁₋₁₂ = 216.2 B ₁₁₋₁₂ = -132.8	0	
N ₂ (group 13)	A ₁₋₁₃ = 38.09 B ₁₋₁₃ = 88.19	A ₂₋₁₃ = 83.73 B ₂₋₁₃ = 188.7	A ₃₋₁₃ = 383.6 B ₃₋₁₃ = 375.4	A ₄₋₁₃ = 341.8 B ₄₋₁₃ = 635.2	A ₅₋₁₃ = 30.88 B ₅₋₁₃ = 37.06	A ₆₋₁₃ = 61.59 B ₆₋₁₃ = 84.92	A ₇₋₁₃ = 185.3 B ₇₋₁₃ = 490.7	A ₈₋₁₃ = 343.8 B ₈₋₁₃ = 1712	A ₉₋₁₃ = 702.4 B ₉₋₁₃ = 1889	A ₁₀₋₁₃ = 179.5 B ₁₀₋₁₃ = 546.6	A ₁₁₋₁₃ = 331.5 B ₁₁₋₁₃ = 389.8	A ₁₂₋₁₃ = 95.05 B ₁₂₋₁₃ = 255.6	0

	CH ₃ (group 1)	CH ₂ (group 2)	CH (group 3)	C (group 4)	CH ₄ (group 5)	C ₂ H ₆ (group 6)	CH _{aro} (group 7)	C _{aro} (group 8)	C _{fused aromatic rings} (group 9)	CH _{2,cyclic} (group 10)	CH _{cyclic} /C _{cyclic} (group 11)	CO ₂ (group 12)	N ₂ (group 13)
H ₂ S (group 14)	A ₁₋₁₄ = 159.6 B ₁₋₁₄ = 227.8	A ₂₋₁₄ = 136.6 B ₂₋₁₄ = 124.6	A ₃₋₁₄ = 192.5 B ₃₋₁₄ = 562.8	A ₄₋₁₄ = 330.8 B ₄₋₁₄ = -297.2	A ₅₋₁₄ = 181.9 B ₅₋₁₄ = 304.0	A ₆₋₁₄ = 157.2 B ₆₋₁₄ = 217.1	A ₇₋₁₄ = 21.28 B ₇₋₁₄ = 6.177	A ₈₋₁₄ = 9.608 B ₈₋₁₄ = -36.72	A ₉₋₁₄ = 9.608 B ₉₋₁₄ = -36.72	A ₁₀₋₁₄ = 117.4 B ₁₀₋₁₄ = 166.4	A ₁₁₋₁₄ = 71.37 B ₁₁₋₁₄ = -127.7	A ₁₂₋₁₄ = 134.9 B ₁₂₋₁₄ = 201.4	A ₁₃₋₁₄ = 319.5 B ₁₃₋₁₄ = 550.1
SH (group 15)	A ₁₋₁₅ = 789.6 B ₁₋₁₅ = 1829	A ₂₋₁₅ = 439.9 B ₂₋₁₅ = 504.8	A ₃₋₁₅ = 374.0 B ₃₋₁₅ = 520.9	A ₄₋₁₅ = 685.9 B ₄₋₁₅ = 1547	A ₅₋₁₅ = 701.7 B ₅₋₁₅ = 1318	NA	A ₇₋₁₅ = 277.6 B ₇₋₁₅ = 449.5	A ₈₋₁₅ = 1002 B ₈₋₁₅ = -736.4	A ₉₋₁₅ = 1002 B ₉₋₁₅ = -736.4	A ₁₀₋₁₅ = 493.1 B ₁₀₋₁₅ = 832.1	A ₁₁₋₁₅ = 463.2 B ₁₁₋₁₅ = -337.7	NA	NA
H ₂ O (group 16)	A ₁₋₁₆ = 3557 B ₁₋₁₆ = 11195	A ₂₋₁₆ = 4324 B ₂₋₁₆ = 12126	A ₃₋₁₆ = 971.4 B ₃₋₁₆ = 567.6	NA	A ₅₋₁₆ = 2265 B ₅₋₁₆ = 4722	A ₆₋₁₆ = 2333 B ₆₋₁₆ = 5147	A ₇₋₁₆ = 2268 B ₇₋₁₆ = 6218	A ₈₋₁₆ = 543.5 B ₈₋₁₆ = 411.8	A ₉₋₁₆ = 1340 B ₉₋₁₆ = -65.88	A ₁₀₋₁₆ = 4211 B ₁₀₋₁₆ = 13031	A ₁₁₋₁₆ = 244.0 B ₁₁₋₁₆ = -60.39	A ₁₂₋₁₆ = 559.3 B ₁₂₋₁₆ = 277.9	A ₁₃₋₁₆ = 2574 B ₁₃₋₁₆ = 5490
C ₂ H ₄ (group 17)	A ₁₋₁₇ = 7.892 B ₁₋₁₇ = 35.00	A ₂₋₁₇ = 59.71 B ₂₋₁₇ = 82.35	A ₃₋₁₇ = 147.9 B ₃₋₁₇ = -55.59	A ₄₋₁₇ = 366.8 B ₄₋₁₇ = -219.3	A ₅₋₁₇ = 19.22 B ₅₋₁₇ = 33.29	A ₆₋₁₇ = 7.549 B ₆₋₁₇ = 20.93	A ₇₋₁₇ = 25.74 B ₇₋₁₇ = 78.92	A ₈₋₁₇ = 97.80 B ₈₋₁₇ = 67.94	A ₉₋₁₇ = 209.7 B ₉₋₁₇ = 3819	A ₁₀₋₁₇ = 35.34 B ₁₀₋₁₇ = 52.50	A ₁₁₋₁₇ = 297.2 B ₁₁₋₁₇ = -647.2	A ₁₂₋₁₇ = 73.09 B ₁₂₋₁₇ = 106.7	A ₁₃₋₁₇ = 45.30 B ₁₃₋₁₇ = 92.65
CH _{2,alkenic} /CH _{alkenic} (group 18)	A ₁₋₁₈ = 48.73 B ₁₋₁₈ = 44.27	A ₂₋₁₈ = 9.608 B ₂₋₁₈ = 50.79	A ₃₋₁₈ = 84.76 B ₃₋₁₈ = 193.2	A ₄₋₁₈ = 181.2 B ₄₋₁₈ = 419.0	A ₅₋₁₈ = 48.73 B ₅₋₁₈ = 68.29	A ₆₋₁₈ = 26.77 B ₆₋₁₈ = -5.147	A ₇₋₁₈ = 9.951 B ₇₋₁₈ = 19.90	A ₈₋₁₈ = -48.38 B ₈₋₁₈ = 27.79	A ₉₋₁₈ = 669.8 B ₉₋₁₈ = 589.5	A ₁₀₋₁₈ = -15.44 B ₁₀₋₁₈ = 24.36	A ₁₁₋₁₈ = 260.1 B ₁₁₋₁₈ = 134.9	A ₁₂₋₁₈ = 60.74 B ₁₂₋₁₈ = 183.9	A ₁₃₋₁₈ = 59.71 B ₁₃₋₁₈ = 227.2
C _{alkenic} (group 19)	A ₁₋₁₉ = 102.6 B ₁₋₁₉ = 260.1	A ₂₋₁₉ = 64.85 B ₂₋₁₉ = 51.82	A ₃₋₁₉ = 91.62 B ₃₋₁₉ = 54.90	NA	NA	NA	A ₇₋₁₉ = -16.47 B ₇₋₁₉ = 61.42	A ₈₋₁₉ = 343.1 B ₈₋₁₉ = 880.2	NA	A ₁₀₋₁₉ = 159.6 B ₁₀₋₁₉ = 140.7	NA	A ₁₂₋₁₉ = 74.81 B ₁₂₋₁₉ = -266.6	A ₁₃₋₁₉ = 541.5 B ₁₃₋₁₉ = 94.71
CH _{cycloalkenic} /C _{cycloalkenic} (group 20)	A ₁₋₂₀ = 47.01 B ₁₋₂₀ = 169.5	A ₂₋₂₀ = 34.31 B ₂₋₂₀ = 51.13	NA	NA	NA	NA	A ₇₋₂₀ = 3.775 B ₇₋₂₀ = 1.716	A ₈₋₂₀ = 242.9 B ₈₋₂₀ = -7.206	NA	A ₁₀₋₂₀ = 31.91 B ₁₀₋₂₀ = 69.32	A ₁₁₋₂₀ = 151.3 B ₁₁₋₂₀ = 2.745	A ₁₂₋₂₀ = 87.85 B ₁₂₋₂₀ = 66.91	NA
H ₂ (group 21)	A ₁₋₂₁ = 174.0 B ₁₋₂₁ = 239.5	A ₂₋₂₁ = 155.4 B ₂₋₂₁ = 240.9	A ₃₋₂₁ = 326.0 B ₃₋₂₁ = 287.9	A ₄₋₂₁ = 548.3 B ₄₋₂₁ = 2343	A ₅₋₂₁ = 156.1 B ₅₋₂₁ = 92.99	A ₆₋₂₁ = 137.6 B ₆₋₂₁ = 150.0	A ₇₋₂₁ = 288.9 B ₇₋₂₁ = 189.1	A ₈₋₂₁ = 400.1 B ₈₋₂₁ = 1201	A ₉₋₂₁ = 602.9 B ₉₋₂₁ = 1463	A ₁₀₋₂₁ = 236.1 B ₁₀₋₂₁ = 192.5	A ₁₁₋₂₁ = -51.82 B ₁₁₋₂₁ = 34.31	A ₁₂₋₂₁ = 265.9 B ₁₂₋₂₁ = 268.3	A ₁₃₋₂₁ = 65.20 B ₁₃₋₂₁ = 70.10
C ₂ F ₆ (group 22)	A ₁₋₂₂ = 119.1 B ₁₋₂₂ = 118.4	A ₂₋₂₂ = 105.0 B ₂₋₂₂ = 130.4	NA	NA	NA	A ₆₋₂₂ = 96.08 B ₆₋₂₂ = 123.5	NA	NA	NA	NA	NA	A ₁₂₋₂₂ = 126.6 B ₁₂₋₂₂ = 241.2	NA
CF ₃ (group 23)	A ₁₋₂₃ = 123.2 B ₁₋₂₃ = 133.8	A ₂₋₂₃ = 195.6 B ₂₋₂₃ = 199.0	A ₃₋₂₃ = 531.5 B ₃₋₂₃ = -1945	A ₄₋₂₃ = 413.1 B ₄₋₂₃ = 975.2	NA	A ₆₋₂₃ = 87.16 B ₆₋₂₃ = 143.8	A ₇₋₂₃ = 680.1 B ₇₋₂₃ = 421.7	A ₈₋₂₃ = 733.0 B ₈₋₂₃ = 866.8	NA	A ₁₀₋₂₃ = 216.2 B ₁₀₋₂₃ = 343.1	NA	A ₁₂₋₂₃ = 156.5 B ₁₂₋₂₃ = -116.0	NA
CF ₂ (group 24)	A ₁₋₂₄ = 58.33 B ₁₋₂₄ = 65.20	A ₂₋₂₄ = 58.33 B ₂₋₂₄ = 68.63	A ₃₋₂₄ = -122.8 B ₃₋₂₄ = 458.8	A ₄₋₂₄ = 479.0 B ₄₋₂₄ = 1430	NA	A ₆₋₂₄ = 79.27 B ₆₋₂₄ = 15.10	A ₇₋₂₄ = -31.57 B ₇₋₂₄ = 43.24	A ₈₋₂₄ = -8.922 B ₈₋₂₄ = 5.147	NA	A ₁₀₋₂₄ = 42.55 B ₁₀₋₂₄ = -68.63	NA	A ₁₂₋₂₄ = 125.2 B ₁₂₋₂₄ = 340.1	NA
CF _{2,double bond} or CF _{double bond} (group 25)	A ₁₋₂₅ = -12.29 B ₁₋₂₅ = 16.54	NA	NA	NA	NA	A ₆₋₂₅ = 95.55 B ₆₋₂₅ = -231.1	A ₇₋₂₅ = -274.3 B ₇₋₂₅ = -411.7	A ₈₋₂₅ = 78.62 B ₈₋₂₅ = -108.0	NA	NA	NA	A ₁₂₋₂₅ = 36.25 B ₁₂₋₂₅ = 63.49	NA
C ₂ H ₄ F ₂ (group 26)	A ₁₋₂₆ = 128.3 B ₁₋₂₆ = 292.4	A ₂₋₂₆ = 107.1 B ₂₋₂₆ = 119.8	A ₃₋₂₆ = 143.8 B ₃₋₂₆ = 15.78	NA	NA	NA	NA	NA	NA	NA	NA	A ₁₂₋₂₆ = 48.73 B ₁₂₋₂₆ = 751.1	NA
C ₂ H ₂ F ₄ (group 27)	A ₁₋₂₇ = 158.5 B ₁₋₂₇ = 356.5	A ₂₋₂₇ = 86.47 B ₂₋₂₇ = -40.49	A ₃₋₂₇ = 121.5 B ₃₋₂₇ = -44.61	NA	NA	A ₆₋₂₇ = 72.40 B ₆₋₂₇ = -305.4	NA	NA	NA	NA	NA	A ₁₂₋₂₇ = 29.51 B ₁₂₋₂₇ = 89.90	NA

	H ₂ S (group 14)	SH (group 15)	H ₂ O (group 16)	C ₂ H ₄ (group 17)	CH ₂ ,alkenic /CH _{alkenic} (group 18)	C _{alkenic} (group 19)	CH _{cycloalkenic} /C _{cycloalkenic} (group 20)	H ₂ (group 21)	C ₂ F ₆ (group 22)	CF ₃ (group 23)	CF ₂ (group 24)	CF ₂ ,double bond or CF _{double bond} (group 25)	C ₂ H ₄ F ₂ (group 26)	C ₂ H ₂ F ₄ (group 27)
H ₂ S (group 14)	0	-	-	-	-	-	-	-	-	-	-	-	-	-
SH (group 15)	A ₁₄₋₁₅ = -157.8 B ₁₄₋₁₅ = 153.7	0	-	-	-	-	-	-	-	-	-	-	-	-
H ₂ O (group 16)	A ₁₄₋₁₆ = 603.9 B ₁₄₋₁₆ = 599.1	A ₁₅₋₁₆ = 30.88 B ₁₅₋₁₆ = -113.6	0	-	-	-	-	-	-	-	-	-	-	-
C ₂ H ₄ (group 17)	NA	NA	A ₁₆₋₁₇ = 1650 B ₁₆₋₁₇ = 1661	0	-	-	-	-	-	-	-	-	-	-
CH ₂ ,alkenic /CH _{alkenic} (group 18)	NA	NA	A ₁₆₋₁₈ = 2243 B ₁₆₋₁₈ = 5199	A ₁₇₋₁₈ = 14.76 B ₁₇₋₁₈ = 11.32	0	-	-	-	-	-	-	-	-	-
C _{alkenic} (group 19)	NA	NA	NA	A ₁₇₋₁₉ = -518.2 B ₁₇₋₁₉ = 6815	A ₁₈₋₁₉ = 24.71 B ₁₈₋₁₉ = 121.8	0	-	-	-	-	-	-	-	-
CH _{cycloalkenic} /C _{cycloalkenic} (group 20)	NA	NA	NA	A ₁₇₋₂₀ = -98.83 B ₁₇₋₂₀ = 1809	A ₁₈₋₂₀ = 14.07 B ₁₈₋₂₀ = -12.35	A ₁₉₋₂₀ = 23.68 B ₁₉₋₂₀ = 87.50	0	-	-	-	-	-	-	-
H ₂ (group 21)	A ₁₄₋₂₁ = 145.8 B ₁₄₋₂₁ = 823.5	NA	A ₁₆₋₂₁ = 830.8 B ₁₆₋₂₁ = -137.9	A ₁₇₋₂₁ = 151.3 B ₁₇₋₂₁ = 165.1	A ₁₈₋₂₁ = 175.7 B ₁₈₋₂₁ = 373.0	A ₁₉₋₂₁ = 621.4 B ₁₉₋₂₁ = 873.6	A ₂₀₋₂₁ = 460.8 B ₂₀₋₂₁ = 2167	0	-	-	-	-	-	-
C ₂ F ₆ (group 22)	NA	NA	NA	NA	A ₁₈₋₂₂ = 124.9 B ₁₈₋₂₂ = 219.6	NA	NA	NA	0	-	-	-	-	-
CF ₃ (group 23)	NA	NA	NA	A ₁₇₋₂₃ = 453.0 B ₁₇₋₂₃ = -611.5	A ₁₈₋₂₃ = 155.4 B ₁₈₋₂₃ = 154.4	NA	A ₂₀₋₂₃ = 1232 B ₂₀₋₂₃ = -495.5	NA	A ₂₂₋₂₃ = -14.47 B ₂₂₋₂₃ = -87.05	0	-	-	-	-
CF ₂ (group 24)	NA	NA	NA	NA	A ₁₈₋₂₄ = 155.4 B ₁₈₋₂₄ = 154.4	NA	NA	NA	NA	A ₂₃₋₂₄ = 0.000 B ₂₃₋₂₄ = 0.000	0	-	-	-
CF ₂ ,double bond or CF _{double bond} (group 25)	NA	NA	NA	A ₁₇₋₂₅ = -132.7 B ₁₇₋₂₅ = 548.3	A ₁₈₋₂₅ = 88.21 B ₁₈₋₂₅ = 12.87	NA	NA	NA	A ₂₂₋₂₅ = 55.90 B ₂₂₋₂₅ = -193.3	A ₂₃₋₂₅ = 17.55 B ₂₃₋₂₅ = -92.99	NA	0	-	-
C ₂ H ₄ F ₂ (group 26)	NA	NA	NA	NA	A ₁₈₋₂₆ = 76.86 B ₁₈₋₂₆ = -145.5	NA	NA	NA	NA	A ₂₃₋₂₆ = 113.2 B ₂₃₋₂₆ = 247.1	A ₂₄₋₂₆ = 120.1 B ₂₄₋₂₆ = 264.2	NA	0	-
C ₂ H ₂ F ₄ (group 27)	NA	NA	NA	NA	A ₁₈₋₂₇ = 64.51 B ₁₈₋₂₇ = -41.86	NA	NA	NA	A ₂₂₋₂₇ = 60.74 B ₂₂₋₂₇ = 217.6	A ₂₃₋₂₇ = 28.14 B ₂₃₋₂₇ = 8.235	A ₂₄₋₂₇ = 229.9 B ₂₄₋₂₇ = 259.1	NA	A ₂₆₋₂₇ = -4.118 B ₂₆₋₂₇ = 4.118	0

Table 2. List of the 35 pure components involved in this study.

Component	Short name
ethane	2
propane	3
n-butane	4
n-pentane	5
n-hexane	6
n-heptane	7
n-octane	8
n-nonane	9
2-methylpropane (isobutane)	2m3
2-methylbutane	2m4
3-methylheptane	3m7
2,2,4-trimethylpentane (isooctane)	224m5
benzene	B
methylbenzene (toluene)	mB
cyclopentane	C5
cyclohexane	C6
carbon dioxide	CO ₂
ethylene	a2
propene	a3
1-butene	1a4
cyclohexene	aC6
hexafluoroethane	R116
octafluoropropane	R218
1,1,1,3,3,3-hexafluoropropane	R236fa
3,3,3-trifluoro-1-propene	R1243
perfluorobutane	R610
1,1,1,3,3-pentafluorobutane	R365mfc
Perfluoro-n-pentane	C ₅ F ₁₂
Perfluoro-n-hexane	C ₆ F ₁₄
Perfluoro-n-heptane	C ₇ F ₁₆
(trifluoromethyl)benzene	FmB
Perfluoro-n-octane	C ₈ F ₁₈
hexafluoropropylene	R1216
1,1-difluoroethane	R152a
1,1,1,2-tetrafluoroethane	R134a

Table 3. Binary systems database.

Binary system (1 st compound- 2 nd compound)	Temperature range (K)	Pressure range (bar)	x_1 range (1 st compound liquid mole fraction)	y_1 range (1 st compound gas mole fraction)	Number of bubble points (T,p,x)	Number of dew points (T,p,y)	Number of binary critical points (T_{cm}, P_{cm}, x_c)	References
R116-3	263.30-323.19	4.53-38.51	0.0180-0.9610	0.1250-0.9630	61	61	0	[5]
R116-4	273.27-323.19	2.99-37.42	0.0112-0.9322	0.2600-0.9589	48	48	0	Personal communication by Pr. C. Coquelet and D. Ramjugernath
R116-5	288.25-296.24	3.07-29.94	0.0186-0.9517	0.7639-0.9853	17	17	0	Personal communication by Pr. C. Coquelet and D. Ramjugernath
R116-6	288.24-296.22	3.12-70.40	0.0193-0.8475	0.9316-0.9839	20	16	0	Personal communication by Pr. C. Coquelet and D. Ramjugernath
2-R116	189.31-296.23	1.44-44.55	0.0270-0.9923	0.0377-0.9892	113	114	0	[89, 90] and Personal communication by Pr. C. Coquelet and D. Ramjugernath
CO ₂ -R116	220.95-296.72	5.96-64.48	0.0218-0.9910	0.0253-0.9904	88	79	0	[4, 47, 79, 80]
R116-a3	251.00-275.00	3.56-19.62	0.0118-0.8363	0.1082-0.8484	13	13	0	[63]
3-R218	203.50-360.40	0.23-39.94	0.0537-0.9217	0.1162-0.9074	30	0	6	[55, 74]
R218-4	227.80-227.80	0.46-0.72	0.0470-0.8621		7	0	0	[55]
3-R236fa	283.13-323.26	2.16-17.50	0.0286-0.9734	0.2061-0.9670	43	43	0	[45]
3-R610	312.92-342.94	7.26-26.05	0.0530-0.9650	0.1820-0.9640	36	36	0	[91]
R610-4	233.23-259.95	0.21-1.00	0.0270-0.9550	0.1780-0.8160	45	45	0	[71]
C ₇ F ₁₂ -5	247.30-403.35	0.13-18.01	0.0140-0.9500	0.1403-0.8310	59	59	0	[42, 82]
3-C ₆ F ₁₄	372.57-443.20	22.08-39.46	0.1225-0.9088	0.1225-0.9088	0	0	6	[74]
C ₆ F ₁₄ -6	298.15-492.57	0.35-29.16	0.0372-0.9597	0.0980-0.8988	38	38	5	[51, 74]
3-C ₇ F ₁₆	377.63-468.09	21.98-41.24	0.0940-0.9080	0.0940-0.9080	0	0	6	[61]
4-C ₇ F ₁₆	420.80-467.26	19.74-33.58	0.1300-0.9160	0.1300-0.9160	0	0	5	[61]
5-C ₇ F ₁₆	449.42-460.29	21.62-30.35	0.2910-0.9130	0.2910-0.9130	0	0	5	[61]
6-C ₇ F ₁₆	464.74-493.42	19.00-27.88	0.1300-0.9040	0.1300-0.9040	0	0	7	[61]
C ₇ F ₁₆ -7	298.16-522.07	0.13-26.31	0.0340-0.9440	0.0960-0.9000	28	16	7	[43, 53, 76]
C ₇ F ₁₆ -8	475.79-548.83	17.51-24.99	0.0990-0.9460	0.0990-0.9460	0	0	6	[61]
C ₇ F ₁₆ -9	484.32-564.66	17.57-24.28	0.1570-0.8680	0.1570-0.8680	0	0	5	[61]
2m3-R236fa	303.68-303.68	3.90-5.35	0.0612-0.9579	0.2007-0.8922	13	13	0	[46]
C ₇ F ₁₆ -3m7	333.15-353.15	0.41-1.02	0.0912-0.9140		20	0	0	[76]
2m4-R365mfc	363.12-413.90	5.22-18.99	0.0191-0.9613	0.0375-0.9308	47	47	0	[92]
C ₇ F ₁₆ -224m5	303.15-343.15	0.10-0.85	0.0119-0.9620	0.1082-0.8655	36	36	0	[75]
2-R218	188.30-188.30	0.48-1.19	0.0958-0.9054		8	0	0	[55]
2-R610	263.14-353.14	1.94-47.40	0.0300-0.9590	0.1450-0.9890	84	84	4	[3]
2-C ₇ F ₁₆	341.89-468.94	22.04-65.93	0.1030-0.8910	0.1030-0.8910	0	0	5	[61]
B-FmB	333.15-373.91	0.28-1.01	0.0350-0.9489	0.0745-0.9692	49	49	0	[59, 66]
FmB-mB	375.23-383.40	1.01-1.01	0.0288-0.9612	0.0445-0.9649	14	14	0	[59]
R218-B	297.21-298.42	1.01-1.01	0.0021-0.0021		2	0	0	[53]
C ₇ F ₁₆ -FmB	343.15-353.15	0.53-1.04	0.0036-0.9551	0.0492-0.9173	22	22	0	[66]
R218-C6	280.15-306.35	1.01-1.01	0.0047-0.0068		5	0	0	[72]
R365mfc-C5	298.15-298.15	0.57-0.64	0.2104-0.9791		7	0	0	[73]
CO ₂ -R610	263.15-352.98	1.83-74.23	0.0218-0.9600	0.2418-0.9830	83	83	4	[8]
CO ₂ -C ₆ F ₁₄	298.00-313.00	6.90-64.80	0.1460-0.9890		25	0	0	[62, 68]
CO ₂ -C ₇ F ₁₆	292.15-303.15	1.01-1.01	0.0170-0.0207		4	0	0	[64]
CO ₂ -C ₈ F ₁₈	293.15-353.15	5.30-108.90	0.1040-0.9600		82	0	0	[49]
a2-R1243	283.10-375.10	9.80-62.90	0.0200-0.9040	0.2550-0.9700	33	33	4	[88]

1a4-R610	312.92-342.93	4.93-14.79	0.0580-0.9520	0.1770-0.7440	38	38	0	[91]
aC6-FmB	333.15-353.15	0.29-0.93	0.0686-0.9913	0.1661-0.9919	19	19	0	[66]
2-R1216	282.93-322.89	6.89-45.78	0.0320-0.9500	0.1710-0.9580	50	50	0	[93]
R1216-mB	273.15-313.15	0.87-7.90	0.0854-0.7040		8	0	0	[2]
CO ₂ -R1216	273.15-313.15	4.06-56.20	0.0320-0.7600	0.1990-0.9340	14	14	0	[7]
a2-R1216	233.15-307.38	0.68-45.59	0.0019-0.9650	0.2760-0.9870	50	46	0	[87, 94]
a3-R1216	263.17-353.14	2.98-40.13	0.0380-0.9860	0.0620-0.9830	81	81	0	[6]
R116-R1216	273.15-313.15	5.06-32.98	0.1154-0.8218	0.2537-0.9253	11	11	0	[2]
3-R152a	273.17-293.19	2.83-9.44	0.0142-0.9544	0.0666-0.9161	15	15	0	[83]
R152a-5	303.88-384.61	3.05-29.12	0.1208-0.9150		39	0	0	[54]
R152a-2m3	303.20-333.20	4.82-16.06	0.0492-0.9897	0.1633-0.9857	32	32	0	[70]
CO ₂ -R152a	318.20-347.70	15.33-81.69	0.0859-0.8840	0.2522-0.9054	52	52	3	[44]
a3-R152a	255.00-298.15	2.05-11.84	0.0329-0.9761	0.0721-0.9726	46	46	0	[63, 77]
R218-R152a	210.21-323.51	0.40-16.00	0.0807-0.8236	0.2170-0.7450	61	61	0	[67, 86]
3-R134a	255.00-355.80	2.41-39.48	0.0200-0.9920	0.0370-0.9750	160	146	0	[57, 60, 63, 69, 84]
R134a-4	283.15-333.15	3.83-17.45	0.0170-0.9760	0.1040-0.9650	53	53	0	[58, 60]
R134a-2m3	293.66-323.20	4.26-14.33	0.0301-0.9727	0.1314-0.9550	52	52	0	[46, 70]
2-R134a	306.55-364.35	45.54-50.83	0.1510-0.9620	0.1510-0.9620	0	0	7	[65]
CO ₂ -R134a	252.95-370.25	3.01-74.74	0.0380-0.9420	0.1200-0.9830	50	50	8	[52, 65, 81]
a3-R134a	251.00-313.15	1.52-17.76	0.0398-0.9260	0.1184-0.9060	92	92	0	[56, 63]
R134a-R116	251.00-275.00	1.86-11.71	0.0175-0.7714	0.1818-0.9083	14	14	0	[63]
R134a-R236fa	283.62-356.85	1.91-22.14	0.1101-0.8982	0.2057-0.9475	15	23	0	[46, 48]
R218-R134a	232.15-232.75	1.01-1.01	0.5694-0.6619		5	0	0	[50]
R134a-R152a	255.00-378.15	1.33-40.88	0.0515-0.9777	0.0545-0.9789	77	77	0	[50, 63, 78, 85]
Total number of points:					2214	1938	93	

Figure captions:

- Fig. 1.** Prediction of vapor-liquid equilibria (VLE), liquid-liquid equilibria (LLE) and global phase equilibrium diagram (GPED) for the binary system: (perfluoro-n-pentane(1) + n-pentane(2)) using the *E*-PPR78 model. (+) experimental bubble points, (*) experimental dew points, (○) experimental critical points in red and experimental LLE points in black, (●) critical points of the pure compounds, (△) experimental upper critical solution temperature (UCST), (▲) predicted UCST. Solid line: predicted curves with the *E*-PPR78 model.
- (a) GPED detailing the phase behaviors at temperatures higher than the predicted UCST. Dotted lines highlight the temperatures of the phase diagrams represented in Fig. 1.b
- (b) VLE phase diagrams at four different temperatures higher than the predicted UCST: $T_1 = 333.14 \text{ K}$ ($k_{ij} = 0.1415$), $T_2 = 353.17 \text{ K}$ ($k_{ij} = 0.1471$), $T_3 = 378.31 \text{ K}$ ($k_{ij} = 0.1543$), $T_4 = 403.35 \text{ K}$ ($k_{ij} = 0.1618$).
- (c) LLE phase diagram and VLE phase diagrams under three different pressures: $P_1 = 0.20 \text{ bar}$, $P_2 = 0.50 \text{ bar}$, $P_3 = 1.00 \text{ bar}$.
- (d) GPED detailing the phase behaviors at relatively low temperatures. Dotted lines highlight the temperatures of the phase diagrams represented in Fig. 1.e
- (e) VLE phase diagrams at five relatively low temperatures: $T_1 = 262.40 \text{ K}$ ($k_{ij} = 0.1227$), $T_2 = 278.60 \text{ K}$ ($k_{ij} = 0.1269$), $T_3 = 283.10 \text{ K}$ ($k_{ij} = 0.1281$), $T_4 = 288.20 \text{ K}$ ($k_{ij} = 0.1294$), $T_5 = 292.90 \text{ K}$ ($k_{ij} = 0.1307$).
- Fig. 2.** Prediction of isothermal phase diagrams for the three binary systems: (ethane(1) + hexafluoroethane(2)), (ethane(1) + perfluoro-n-butane(2)) and (ethane(1) + hexafluoropropylene(2)) using the *E*-PPR78 model. (+) experimental bubble points, (*) experimental dew points. Solid line: predicted curves with the *E*-PPR78 model.
- (a) System (ethane(1) + hexafluoroethane(2)) at seven different temperatures: $T_1 = 189.31 \text{ K}$ ($k_{ij} = 0.1266$), $T_2 = 199.64 \text{ K}$ ($k_{ij} = 0.1271$), $T_3 = 213.06 \text{ K}$ ($k_{ij} = 0.1278$), $T_4 = 228.28 \text{ K}$ ($k_{ij} = 0.1287$), $T_5 = 242.93 \text{ K}$ ($k_{ij} = 0.1297$), $T_6 = 247.63 \text{ K}$ ($k_{ij} = 0.1301$), $T_7 = 253.31 \text{ K}$ ($k_{ij} = 0.1305$).
- (b) System (ethane(1) + hexafluoroethane(2)) at four different temperatures: $T_1 = 273.28 \text{ K}$ ($k_{ij} = 0.1321$), $T_2 = 288.25 \text{ K}$ ($k_{ij} = 0.1333$), $T_3 = 294.22 \text{ K}$ ($k_{ij} = 0.1339$), $T_4 = 296.23 \text{ K}$ ($k_{ij} = 0.1341$).
- (c) System (ethane(1) + perfluoro-n-butane(2)) at seven different temperatures: $T_1 = 263.14 \text{ K}$ ($k_{ij} = 0.1020$), $T_2 = 283.19 \text{ K}$ ($k_{ij} = 0.1061$), $T_3 = 303.20 \text{ K}$ ($k_{ij} = 0.1106$), $T_4 = 308.20 \text{ K}$ ($k_{ij} = 0.1118$), $T_5 = 323.19 \text{ K}$ ($k_{ij} = 0.1156$), $T_6 = 338.20 \text{ K}$ ($k_{ij} = 0.1196$), $T_7 = 353.14 \text{ K}$ ($k_{ij} = 0.1239$).
- (d) System (ethane(1) + hexafluoropropylene(2)) at five different temperatures: $T_1 = 282.93 \text{ K}$ ($k_{ij} = 0.1111$), $T_2 = 293.96 \text{ K}$ ($k_{ij} = 0.1225$), $T_3 = 303.94 \text{ K}$ ($k_{ij} = 0.1341$), $T_4 = 312.90 \text{ K}$ ($k_{ij} = 0.1454$), $T_5 = 322.89 \text{ K}$ ($k_{ij} = 0.1593$).

Fig. 3. Prediction of isothermal phase diagrams for the four binary systems: (propane(1) + 1,1-difluoroethane(2)), (propane(1) + 1,1,1,2-tetrafluoroethane(2)), (propane(1) + perfluoro-n-butane(2)) and (hexafluoroethane(1) + propane(2)) using the *E*-PPR78 model. (+) experimental bubble points, (*) experimental dew points. Solid line: predicted curves with the *E*-PPR78 model.

(a) System (propane(1) + 1,1-difluoroethane(2)) at two different temperatures: $T_1 = 273.17$ K ($k_{ij} = 0.1420$), $T_2 = 293.19$ K ($k_{ij} = 0.1377$).

(b) System (propane(1) + 1,1,1,2-tetrafluoroethane(2)) at six different temperatures: $T_1 = 273.15$ K ($k_{ij} = 0.1671$), $T_2 = 283.15$ K ($k_{ij} = 0.1660$), $T_3 = 293.15$ K ($k_{ij} = 0.1653$), $T_4 = 303.15$ K ($k_{ij} = 0.1649$), $T_5 = 313.15$ K ($k_{ij} = 0.1648$), $T_6 = 323.15$ K ($k_{ij} = 0.1651$).

(c) System (propane(1) + perfluoro-n-butane(2)) at three different temperatures: $T_1 = 312.92$ K ($k_{ij} = 0.1282$), $T_2 = 327.94$ K ($k_{ij} = 0.1318$), $T_3 = 342.94$ K ($k_{ij} = 0.1356$).

(d) System (hexafluoroethane(1) + propane(2)) at six different temperatures: $T_1 = 263.30$ K ($k_{ij} = 0.1374$), $T_2 = 283.25$ K ($k_{ij} = 0.1428$), $T_3 = 291.22$ K ($k_{ij} = 0.1450$), $T_4 = 296.23$ K ($k_{ij} = 0.1464$), $T_5 = 308.21$ K ($k_{ij} = 0.1497$), $T_6 = 323.19$ K ($k_{ij} = 0.1539$).

Fig. 4. Prediction of isothermal phase diagrams for the five binary systems: (hexafluoroethane(1) + n-butane(2)), (1,1,1,2-tetrafluoroethane(1) + n-butane(2)), (hexafluoroethane(1) + n-pentane(2)), (1,1-difluoroethane(1) + n-pentane(2)) and (hexafluoroethane(1) + n-hexane(2)) using the *E*-PPR78 model. (+) experimental bubble points, (*) experimental dew points. Solid line: predicted curves with the *E*-PPR78 model.

(a) System (hexafluoroethane(1) + n-butane(2)) at six different temperatures: $T_1 = 273.27$ K ($k_{ij} = 0.1383$), $T_2 = 288.25$ K ($k_{ij} = 0.1420$), $T_3 = 294.23$ K ($k_{ij} = 0.1435$), $T_4 = 296.22$ K ($k_{ij} = 0.1440$), $T_5 = 308.21$ K ($k_{ij} = 0.1470$), $T_6 = 323.19$ K ($k_{ij} = 0.1509$).

(b) System (1,1,1,2-tetrafluoroethane(1) + n-butane(2)) at four different temperatures: $T_1 = 283.15$ K ($k_{ij} = 0.1453$), $T_2 = 313.15$ K ($k_{ij} = 0.1508$), $T_3 = 323.15$ K ($k_{ij} = 0.1533$), $T_4 = 333.15$ K ($k_{ij} = 0.1562$).

(c) System (hexafluoroethane(1) + n-pentane(2)) at two different temperatures: $T_1 = 288.25$ K ($k_{ij} = 0.1491$), $T_2 = 296.24$ K ($k_{ij} = 0.1511$).

(d) System (1,1-difluoroethane(1) + n-pentane(2)) at five different temperatures: $T_1 = 303.88$ K ($k_{ij} = 0.1297$), $T_2 = 323.73$ K ($k_{ij} = 0.1298$), $T_3 = 343.93$ K ($k_{ij} = 0.1304$), $T_4 = 364.10$ K ($k_{ij} = 0.1314$), $T_5 = 384.61$ K ($k_{ij} = 0.1327$).

(e) System (hexafluoroethane(1) + n-hexane(2)) at $T = 288.24$ K ($k_{ij} = 0.1572$).

Fig. 5. Prediction of isothermal phase diagrams for the four binary systems: (propane(1) + perfluoropropane(2)), (perfluoro-n-butane(1) + n-butane(2)), (perfluoro-n-hexane(1) + n-hexane(2)) and (perfluoro-n-heptane(1) + n-heptane(2)) and prediction of critical loci for fourteen binary systems containing a fluorocompound and an n-alkane using the *E*-PPR78 model. (+) experimental bubble points, (*) experimental dew points, (○) experimental critical points, (●) critical points of the pure compounds. Solid line: predicted curves with the *E*-PPR78 model.

(a) System (propane(1) + perfluoropropane(2)) at three different temperatures: $T_1 = 203.50 \text{ K}$ ($k_{ij} = 0.1261$), $T_2 = 213.60 \text{ K}$ ($k_{ij} = 0.1289$), $T_3 = 223.50 \text{ K}$ ($k_{ij} = 0.1316$).

(b) System (perfluoro-n-butane(1) + n-butane(2)) at five different temperatures: $T_1 = 233.23 \text{ K}$ ($k_{ij} = 0.1202$), $T_2 = 238.45 \text{ K}$ ($k_{ij} = 0.1215$), $T_3 = 246.35 \text{ K}$ ($k_{ij} = 0.1236$), $T_4 = 253.62 \text{ K}$ ($k_{ij} = 0.1255$), $T_5 = 259.95 \text{ K}$ ($k_{ij} = 0.1271$).

(c) System (perfluoro-n-hexane(1) + n-hexane(2)) at three different temperatures: $T_1 = 298.15 \text{ K}$ ($k_{ij} = 0.1319$), $T_2 = 308.15 \text{ K}$ ($k_{ij} = 0.1345$), $T_3 = 318.15 \text{ K}$ ($k_{ij} = 0.1371$).

(d) System (perfluoro-n-heptane(1) + n-heptane(2)) at three different temperatures: $T_1 = 298.16 \text{ K}$ ($k_{ij} = 0.1307$), $T_2 = 318.16 \text{ K}$ ($k_{ij} = 0.1359$), $T_3 = 328.16 \text{ K}$ ($k_{ij} = 0.1385$).

(e-f) Prediction of the critical loci for fourteen binary systems containing a fluorocompound and an n-alkane.

Fig. 6. Prediction of isothermal phase diagrams for the four binary systems: (1,1-difluoroethane(1) + 2-methylpropane(2)), (1,1,1,2-tetrafluoroethane(1) + 2-methylpropane(2)), (perfluoro-n-heptane(1) + 3-methylheptane(2)) and (perfluoro-n-heptane(1) + 2,2,4-trimethylpentane(2)) using the *E*-PPR78 model. (+) experimental bubble points, (*) experimental dew points. Solid line: predicted curves with the *E*-PPR78 model.

(a) System (1,1-difluoroethane(1) + 2-methylpropane(2)) at four different temperatures: $T_1 = 303.20 \text{ K}$ ($k_{ij} = 0.1189$), $T_2 = 313.20 \text{ K}$ ($k_{ij} = 0.1183$), $T_3 = 323.20 \text{ K}$ ($k_{ij} = 0.1180$), $T_4 = 333.20 \text{ K}$ ($k_{ij} = 0.1179$).

(b) System (1,1,1,2-tetrafluoroethane(1) + 2-methylpropane(2)) at three different temperatures: $T_1 = 293.66 \text{ K}$ ($k_{ij} = 0.1563$), $T_2 = 303.20 \text{ K}$ ($k_{ij} = 0.1553$), $T_3 = 323.20 \text{ K}$ ($k_{ij} = 0.1541$).

(c) System (perfluoro-n-heptane(1) + 3-methylheptane (2)) at four different temperatures: $T_1 = 333.15 \text{ K}$ ($k_{ij} = 0.1214$), $T_2 = 338.15 \text{ K}$ ($k_{ij} = 0.1247$), $T_3 = 343.15 \text{ K}$ ($k_{ij} = 0.1283$), $T_4 = 353.15 \text{ K}$ ($k_{ij} = 0.1359$).

(d) System (perfluoro-n-heptane(1) + 2,2,4-trimethylpentane(2)) at three different temperatures: $T_1 = 303.15 \text{ K}$ ($k_{ij} = 0.1266$), $T_2 = 323.15 \text{ K}$ ($k_{ij} = 0.1265$), $T_3 = 343.15 \text{ K}$ ($k_{ij} = 0.1300$).

Fig. 7. Prediction of isothermal phase diagrams for the four binary systems: (benzene(1) + trifluoromethylbenzene(2)), (perfluoro-n-heptane(1) + trifluoromethylbenzene(2)), (cyclohexene(1) + trifluoromethylbenzene(2)) and (hexafluoropropylene(1) + methylbenzene(2)) using the *E*-PPR78 model. (+) experimental bubble points, (*) experimental dew points. Solid line: predicted curves with the *E*-PPR78 model.

(a) System (benzene(1) + trifluoromethylbenzene(2)) at three different temperatures: $T_1 = 333.15 \text{ K}$ ($k_{ij} = -0.0015$), $T_2 = 343.15 \text{ K}$ ($k_{ij} = -0.0009$), $T_3 = 353.15 \text{ K}$ ($k_{ij} = -0.0004$).

(b) System (perfluoro-n-heptane(1) + trifluoromethylbenzene(2)) at two different temperatures: $T_1 = 343.15 \text{ K}$ ($k_{ij} = 0.0818$), $T_2 = 353.15 \text{ K}$ ($k_{ij} = 0.0814$).

(c) System (cyclohexene(1) + trifluoromethylbenzene(2)) at two different temperatures: $T_1 = 333.15 \text{ K}$ ($k_{ij} = 0.0252$), $T_2 = 353.15 \text{ K}$ ($k_{ij} = 0.0316$).

(d) System (hexafluoropropylene(1) + methylbenzene(2)) at two different temperatures: $T_1 = 273.15 \text{ K}$ ($k_{ij} = 0.0403$), $T_2 = 313.15 \text{ K}$ ($k_{ij} = 0.0645$).

Fig. 8. Prediction of isothermal phase diagrams for the three binary systems: (CO₂(1) + hexafluoroethane(2)), (CO₂(1) + perfluoro-n-butane(2)) and (CO₂(1) + perfluoro-n-hexane(2)) using the *E*-PPR78 model. (+) experimental bubble points, (*) experimental dew points. Solid line: predicted curves with the *E*-PPR78 model.

(a) System (CO₂(1) + hexafluoroethane(2)) at three different temperatures: $T_1 = 227.60 \text{ K}$ ($k_{ij} = 0.0870$), $T_2 = 253.29 \text{ K}$ ($k_{ij} = 0.0798$), $T_3 = 273.27 \text{ K}$ ($k_{ij} = 0.0753$).

(b) System (CO₂(1) + hexafluoroethane(2)) at four different temperatures: $T_1 = 283.24 \text{ K}$ ($k_{ij} = 0.0734$), $T_2 = 291.22 \text{ K}$ ($k_{ij} = 0.0720$), $T_3 = 294.22 \text{ K}$ ($k_{ij} = 0.0715$), $T_4 = 296.72 \text{ K}$ ($k_{ij} = 0.0711$).

(c) System (CO₂(1) + perfluoro-n-butane(2)) at seven different temperatures: $T_1 = 263.15 \text{ K}$ ($k_{ij} = 0.0683$), $T_2 = 283.00 \text{ K}$ ($k_{ij} = 0.0761$), $T_3 = 303.12 \text{ K}$ ($k_{ij} = 0.0873$), $T_4 = 308.19 \text{ K}$ ($k_{ij} = 0.0906$), $T_5 = 323.20 \text{ K}$ ($k_{ij} = 0.1016$), $T_6 = 338.20 \text{ K}$ ($k_{ij} = 0.1143$), $T_7 = 352.98 \text{ K}$ ($k_{ij} = 0.1286$).

(d) System (CO₂(1) + perfluoro-n-hexane(2)) at two different temperatures: $T_1 = 298.00 \text{ K}$ ($k_{ij} = 0.0678$), $T_2 = 313.00 \text{ K}$ ($k_{ij} = 0.0712$).

Fig. 9. Prediction of isothermal phase diagrams for the four binary systems: (CO₂(1) + perfluoro-n-octane(2)), (CO₂(1) + hexafluoropropylene(2)), (CO₂(1) + 1,1-difluoroethane(2)) and (CO₂(1) + 1,1,1,2-tetrafluoroethane(2)) and prediction of critical loci for four binary systems using the *E*-PPR78 model. (+) experimental bubble points, (*) experimental dew points, (○) experimental critical points, (●) critical points of the pure compounds. Solid line: predicted curves with the *E*-PPR78 model.

(a) System (CO₂(1) + perfluoro-n-octane(2)) at seven different temperatures: $T_1 = 293.15 \text{ K}$ ($k_{ij} = 0.0661$), $T_2 = 303.15 \text{ K}$ ($k_{ij} = 0.0658$), $T_3 = 313.15 \text{ K}$ ($k_{ij} = 0.0662$), $T_4 = 323.15 \text{ K}$ ($k_{ij} = 0.0672$), $T_5 = 333.15 \text{ K}$ ($k_{ij} = 0.0688$), $T_6 = 343.15 \text{ K}$ ($k_{ij} = 0.0709$), $T_7 = 353.15 \text{ K}$ ($k_{ij} = 0.0737$).

(b) System (CO₂(1) + hexafluoropropylene(2)) at two different temperatures: $T_1 = 273.15 \text{ K}$ ($k_{ij} = 0.0172$), $T_2 = 313.15 \text{ K}$ ($k_{ij} = 0.0327$).

(c) System (CO₂(1) + 1,1-difluoroethane(2)) at three different temperatures: $T_1 = 318.20 \text{ K}$ ($k_{ij} = 0.0080$), $T_2 = 333.00 \text{ K}$ ($k_{ij} = -0.0013$), $T_3 = 347.70 \text{ K}$ ($k_{ij} = -0.0060$).

(d) System (CO₂(1) + 1,1,1,2-tetrafluoroethane(2)) at six different temperatures: $T_1 = 252.95 \text{ K}$ ($k_{ij} = 0.0169$), $T_2 = 272.75 \text{ K}$ ($k_{ij} = 0.0128$), $T_3 = 292.95 \text{ K}$ ($k_{ij} = 0.0094$), $T_4 = 329.60 \text{ K}$ ($k_{ij} = 0.0046$), $T_5 = 339.10 \text{ K}$ ($k_{ij} = 0.0036$), $T_6 = 354.00 \text{ K}$ ($k_{ij} = 0.0021$).

(e) Prediction of the critical loci for four binary systems.

Fig. 10. Prediction of isothermal phase diagrams for the six binary systems: (ethylene(1) + hexafluoropropylene(2)), (hexafluoroethane(1) + propene(2)), (1-butene(1) + perfluoro-n-butane(2)), (propene(1) + 1,1-difluoroethane(2)), (propene(1) + 1,1,1,2-tetrafluoroethane(2)) and (propene(1) + hexafluoropropylene(2)) using the *E*-PPR78 model. (+) experimental bubble points, (*) experimental dew points. Solid line: predicted curves with the *E*-PPR78 model.

(a) System (ethylene(1) + hexafluoropropylene(2)) at six different temperatures: $T_1 = 258.35 \text{ K}$ ($k_{ij} = 0.0828$), $T_2 = 268.24 \text{ K}$ ($k_{ij} = 0.0851$), $T_3 = 278.10 \text{ K}$ ($k_{ij} = 0.0858$), $T_4 = 288.06 \text{ K}$ ($k_{ij} = 0.0846$), $T_5 = 297.42 \text{ K}$ ($k_{ij} = 0.0812$), $T_6 = 307.38 \text{ K}$ ($k_{ij} = 0.0748$).

(b) System (hexafluoroethane(1) + propene(2)) at two different temperatures: $T_1 = 251.00 \text{ K}$ ($k_{ij} = 0.1577$), $T_2 = 275.00 \text{ K}$ ($k_{ij} = 0.1549$).

(c) System (1-butene(1) + perfluoro-n-butane(2)) at three different temperatures: $T_1 = 312.92 \text{ K}$ ($k_{ij} = 0.1826$), $T_2 = 327.93 \text{ K}$ ($k_{ij} = 0.1881$), $T_3 = 342.93 \text{ K}$ ($k_{ij} = 0.1936$).

(d) System (propene(1) + 1,1-difluoroethane(2)) at five different temperatures: $T_1 = 255.00 \text{ K}$ ($k_{ij} = 0.0851$), $T_2 = 265.00 \text{ K}$ ($k_{ij} = 0.0883$), $T_3 = 275.00 \text{ K}$ ($k_{ij} = 0.0923$), $T_4 = 285.00 \text{ K}$ ($k_{ij} = 0.0969$), $T_5 = 298.15 \text{ K}$ ($k_{ij} = 0.1041$).

(e) System (propene(1) + 1,1,1,2-tetrafluoroethane(2)) at five different temperatures: $T_1 = 251.00 \text{ K}$ ($k_{ij} = 0.1051$), $T_2 = 275.00 \text{ K}$ ($k_{ij} = 0.1079$), $T_3 = 293.15 \text{ K}$ ($k_{ij} = 0.1114$), $T_4 = 303.15 \text{ K}$ ($k_{ij} = 0.1137$), $T_5 = 313.15 \text{ K}$ ($k_{ij} = 0.1164$).

(f) System (propene(1) + hexafluoropropylene(2)) at six different temperatures: $T_1 = 263.17 \text{ K}$ ($k_{ij} = 0.0858$), $T_2 = 273.16 \text{ K}$ ($k_{ij} = 0.0878$), $T_3 = 293.12 \text{ K}$ ($k_{ij} = 0.0915$), $T_4 = 313.11 \text{ K}$ ($k_{ij} = 0.0944$), $T_5 = 333.11 \text{ K}$ ($k_{ij} = 0.0961$), $T_6 = 353.14 \text{ K}$ ($k_{ij} = 0.0959$).

Fig. 11. Prediction of isothermal and isobaric curves for the five binary systems: (hexafluoroethane(1) + hexafluoropropylene(2)), (hexafluoroethane(1) + 1,1,1,2-tetrafluoroethane(2)), (1,1,1,2-tetrafluoroethane(1) + 1,1,1,3,3,3-hexafluoropropane(2)), (1,1,1,2-tetrafluoroethane(1) + 1,1-difluoroethane(2)) and (perfluoropropane(1) + 1,1-difluoroethane(2)) using the *E*-PPR78 model. (+) experimental bubble points, (*) experimental dew points. Solid line: predicted curves with the *E*-PPR78 model.

(a) System (hexafluoroethane(1) + hexafluoropropylene(2)) at two different temperatures: $T_1 = 273.15 \text{ K}$ ($k_{ij} = 0.0244$), $T_2 = 313.15 \text{ K}$ ($k_{ij} = 0.0727$).

(b) System (hexafluoroethane(1) + 1,1,1,2-tetrafluoroethane(2)) at two different temperatures: $T_1 = 251.00 \text{ K}$ ($k_{ij} = 0.1192$), $T_2 = 275.00 \text{ K}$ ($k_{ij} = 0.0949$).

(c) System (1,1,1,2-tetrafluoroethane(1) + 1,1,1,3,3,3-hexafluoropropane(2)) at two different temperatures: $T_1 = 283.62 \text{ K}$ ($k_{ij} = -0.0020$), $T_2 = 303.68 \text{ K}$ ($k_{ij} = 0.0038$).

(d) System (1,1,1,2-tetrafluoroethane(1) + 1,1-difluoroethane(2)) at seven different temperatures: $T_1 = 255.00 \text{ K}$ ($k_{ij} = -0.0049$), $T_2 = 275.00 \text{ K}$ ($k_{ij} = -0.0058$), $T_3 = 298.00 \text{ K}$ ($k_{ij} = -0.0069$), $T_4 = 313.15 \text{ K}$ ($k_{ij} = -0.0078$), $T_5 = 323.15 \text{ K}$ ($k_{ij} = -0.0084$), $T_6 = 333.15 \text{ K}$ ($k_{ij} = -0.0090$), $T_7 = 343.15 \text{ K}$ ($k_{ij} = -0.0097$).

(e) System (perfluoropropane(1) + 1,1-difluoroethane(2)) at six different temperatures: $T_1 = 213.15 \text{ K}$ ($k_{ij} = 0.1922$), $T_2 = 233.15 \text{ K}$ ($k_{ij} = 0.1781$), $T_3 = 253.15 \text{ K}$ ($k_{ij} = 0.1664$), $T_4 = 273.15 \text{ K}$ ($k_{ij} = 0.1565$), $T_5 = 293.15 \text{ K}$ ($k_{ij} = 0.1480$), $T_6 = 313.15 \text{ K}$ ($k_{ij} = 0.1407$).

(f) System (perfluoropropane(1) + 1,1-difluoroethane(2)) at five different pressures: $P_1 = 1.00 \text{ bar}$, $P_2 = 4.00 \text{ bar}$, $P_3 = 8.00 \text{ bar}$, $P_4 = 12.00 \text{ bar}$, $P_5 = 16.00 \text{ bar}$.

FIGURE 1

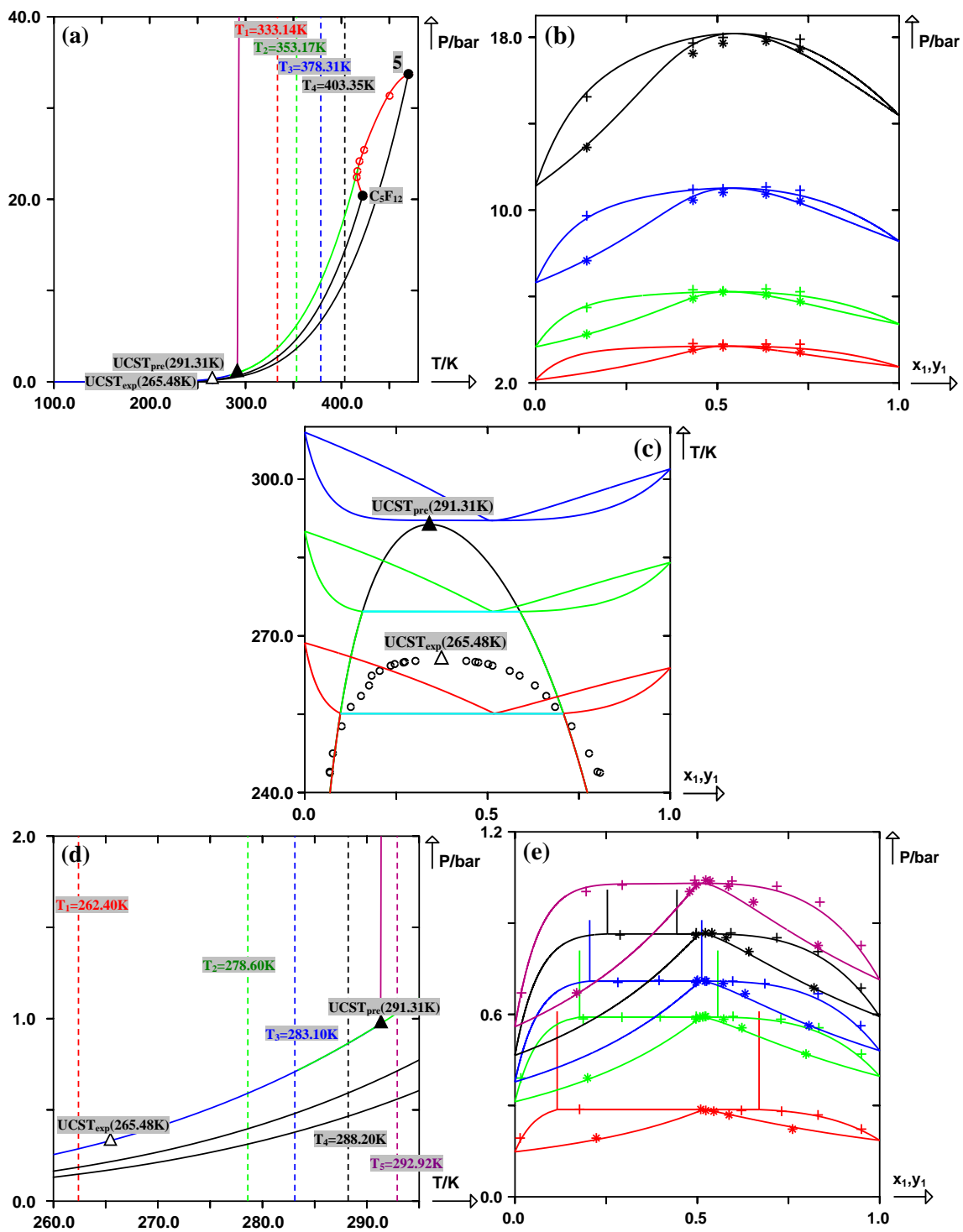


FIGURE 2

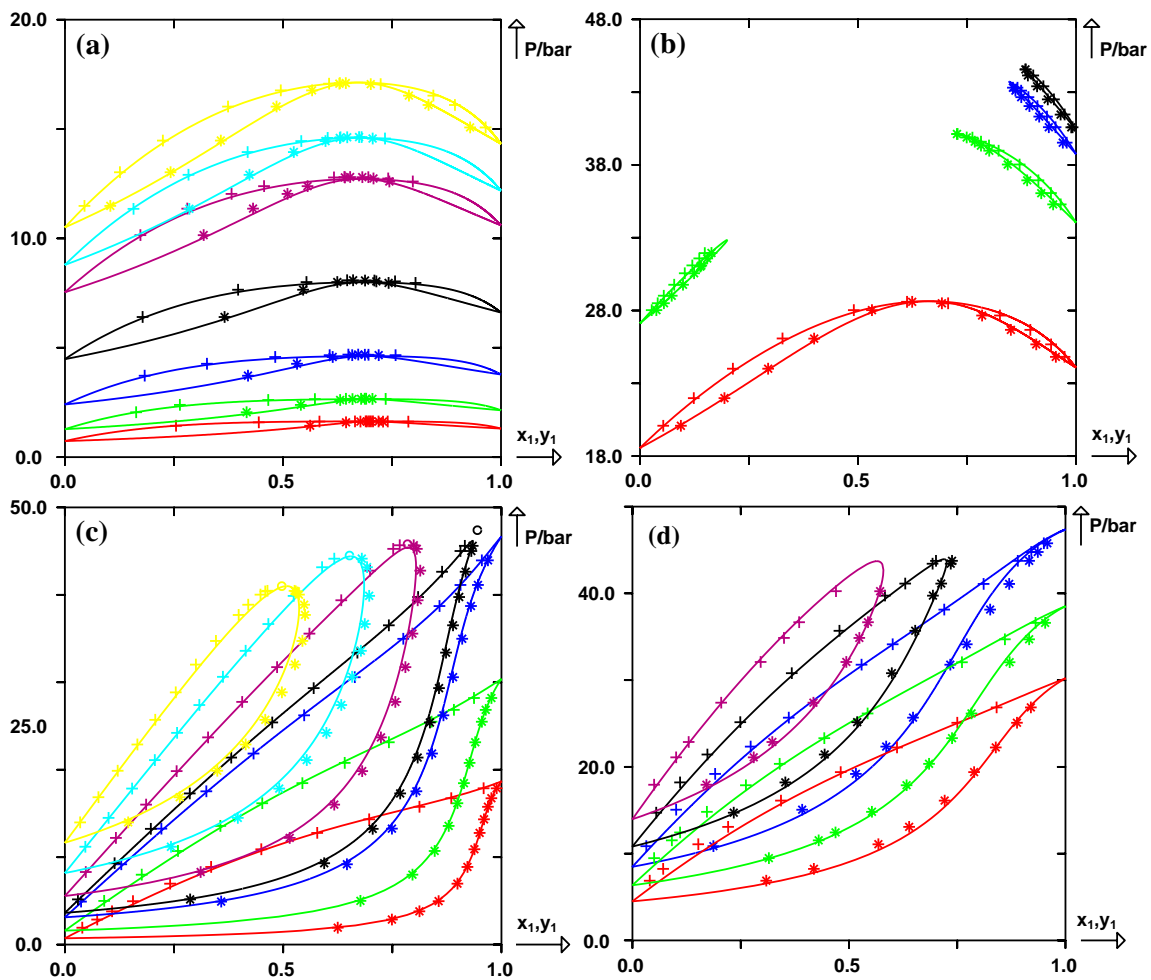


FIGURE 3

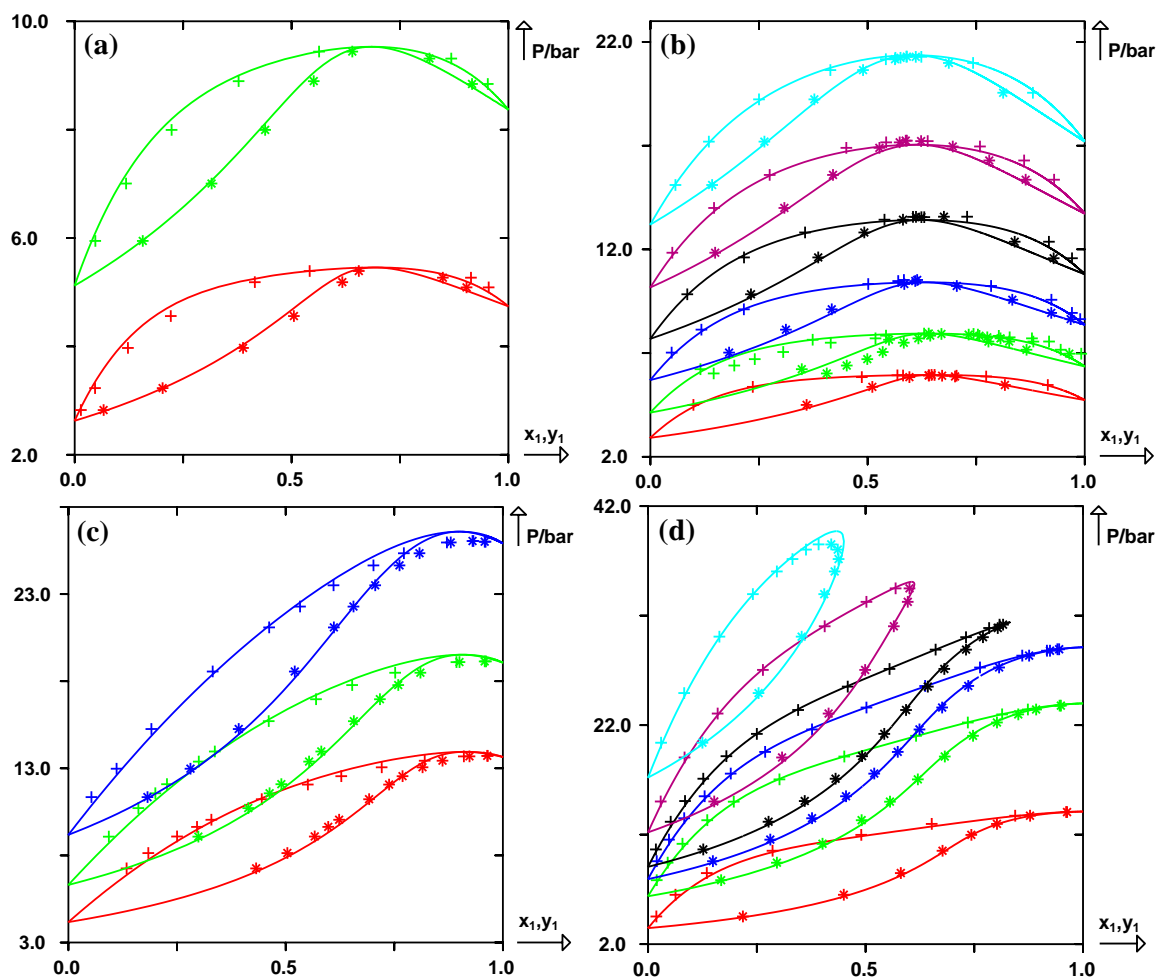


FIGURE 4

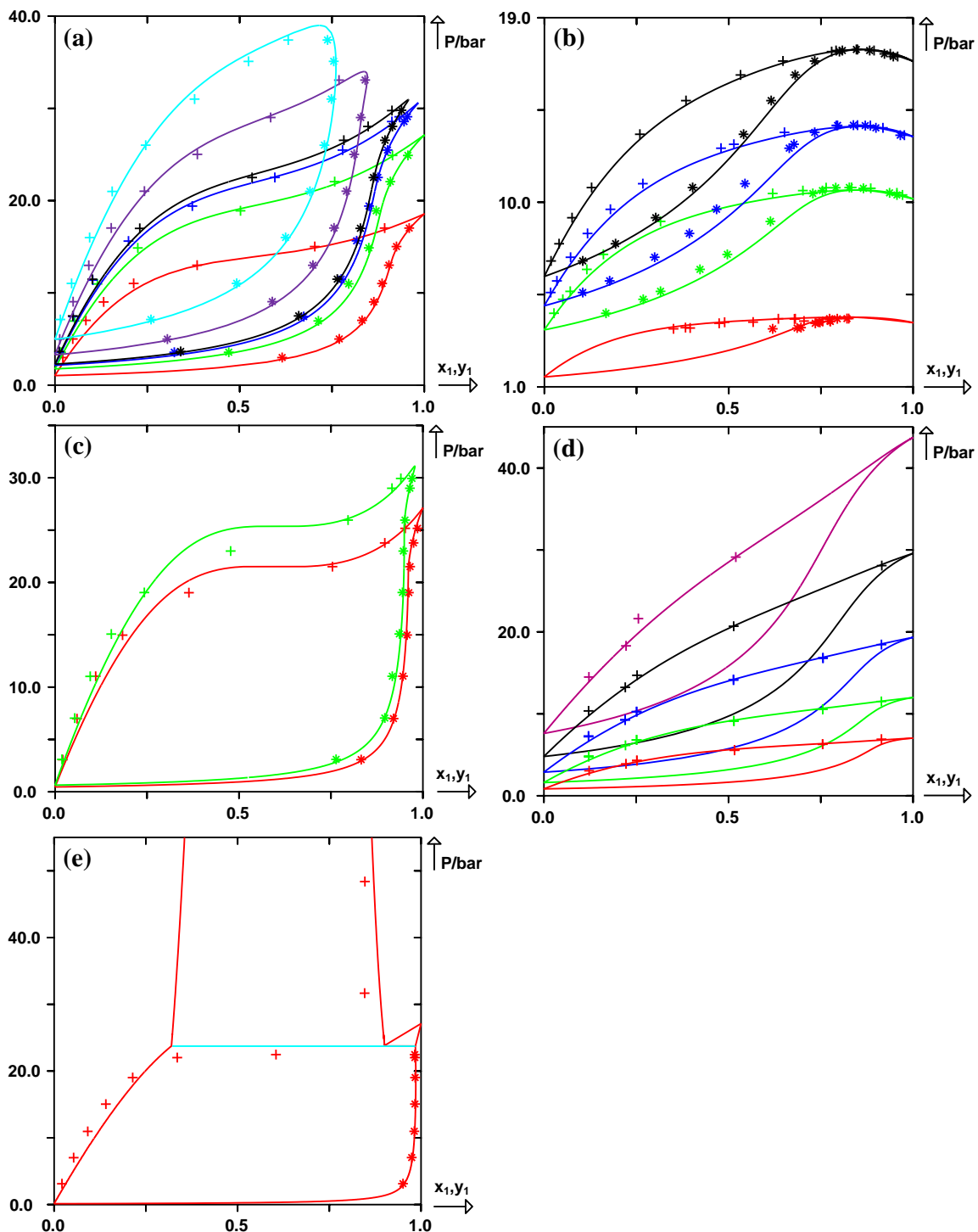


FIGURE 5

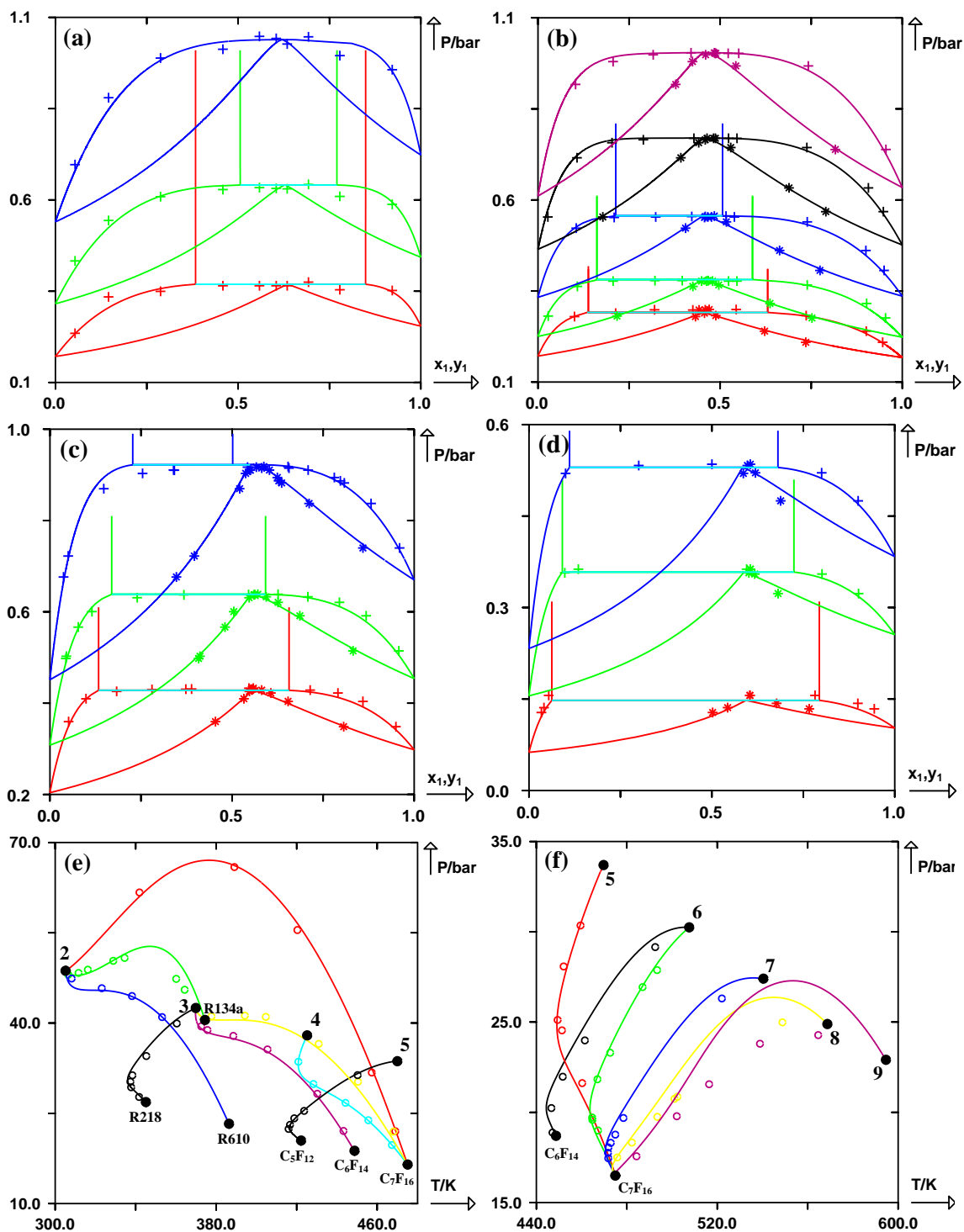


FIGURE 6

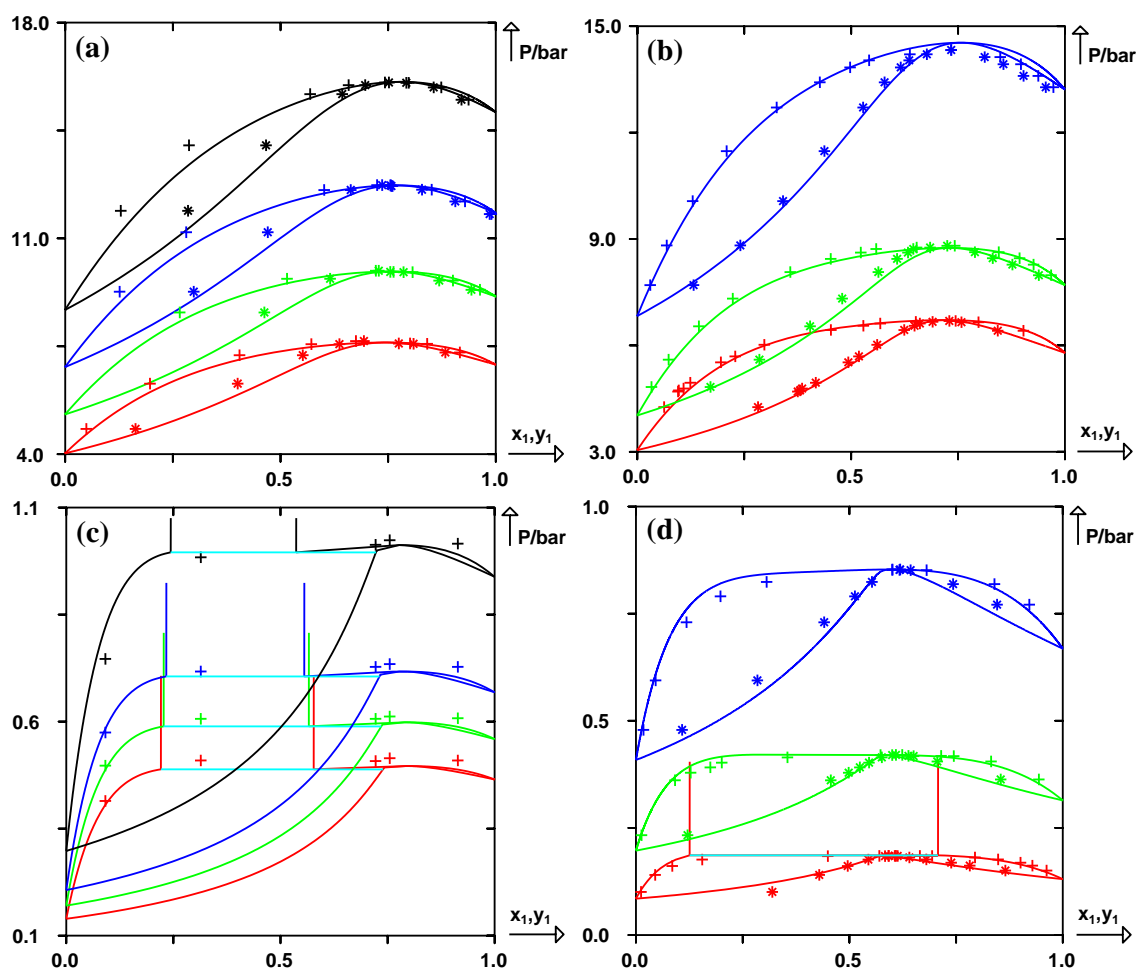


FIGURE 7

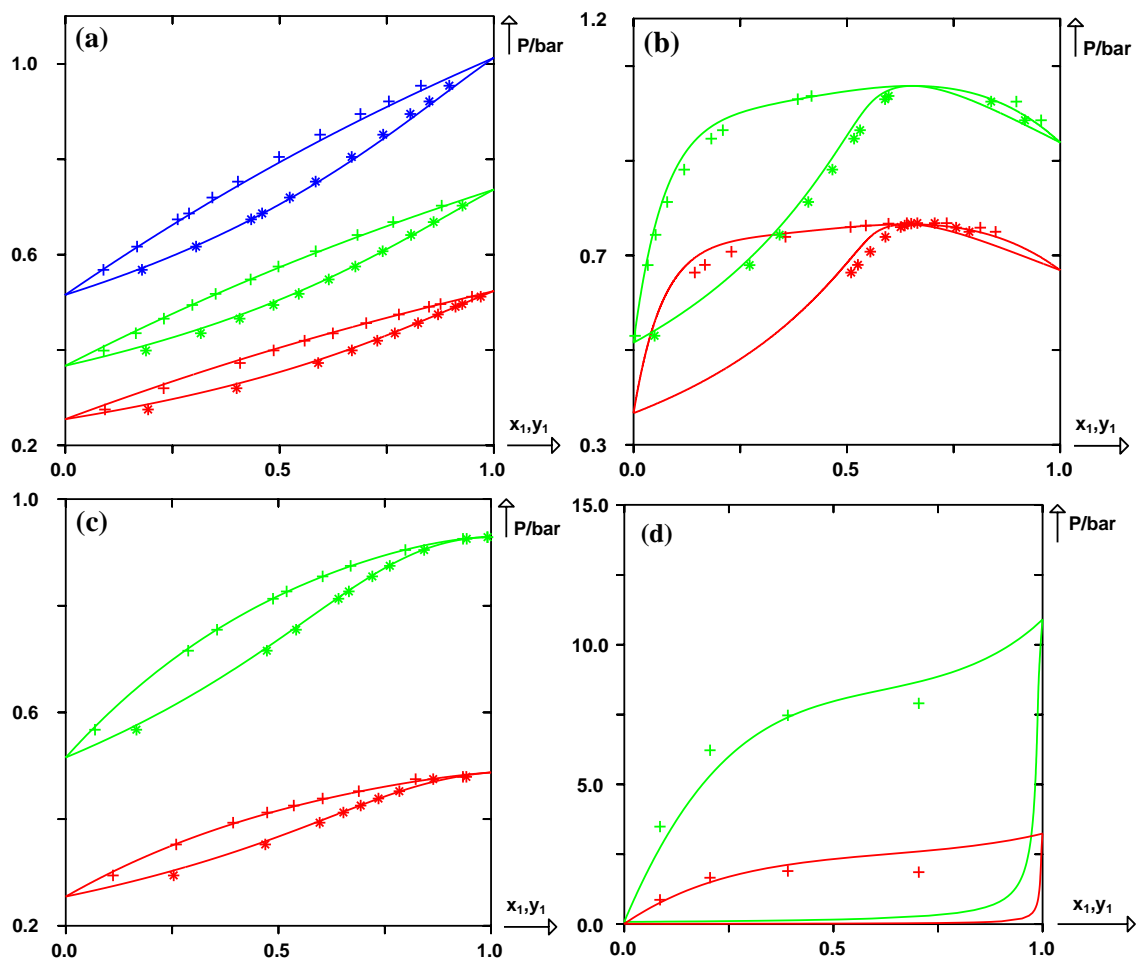


FIGURE 8

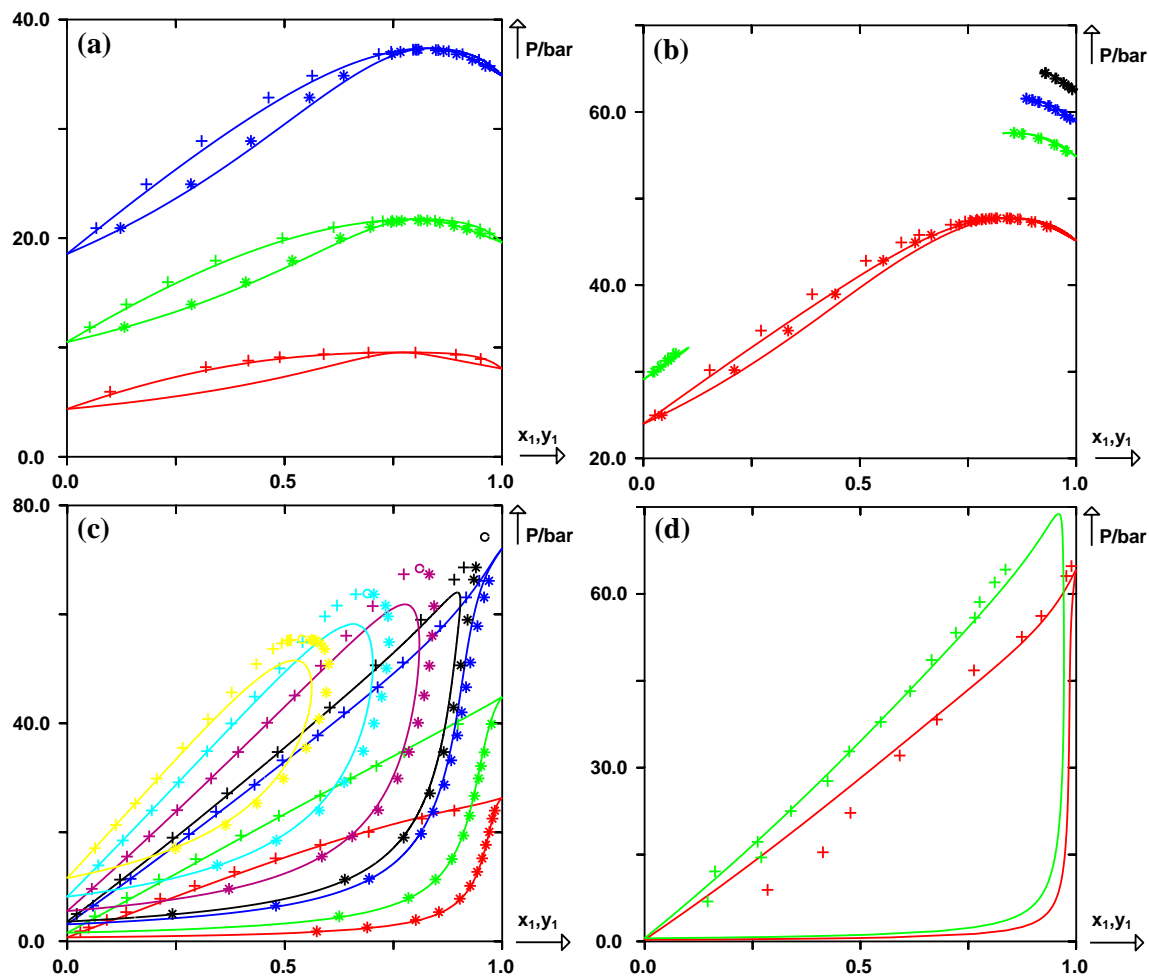


FIGURE 9

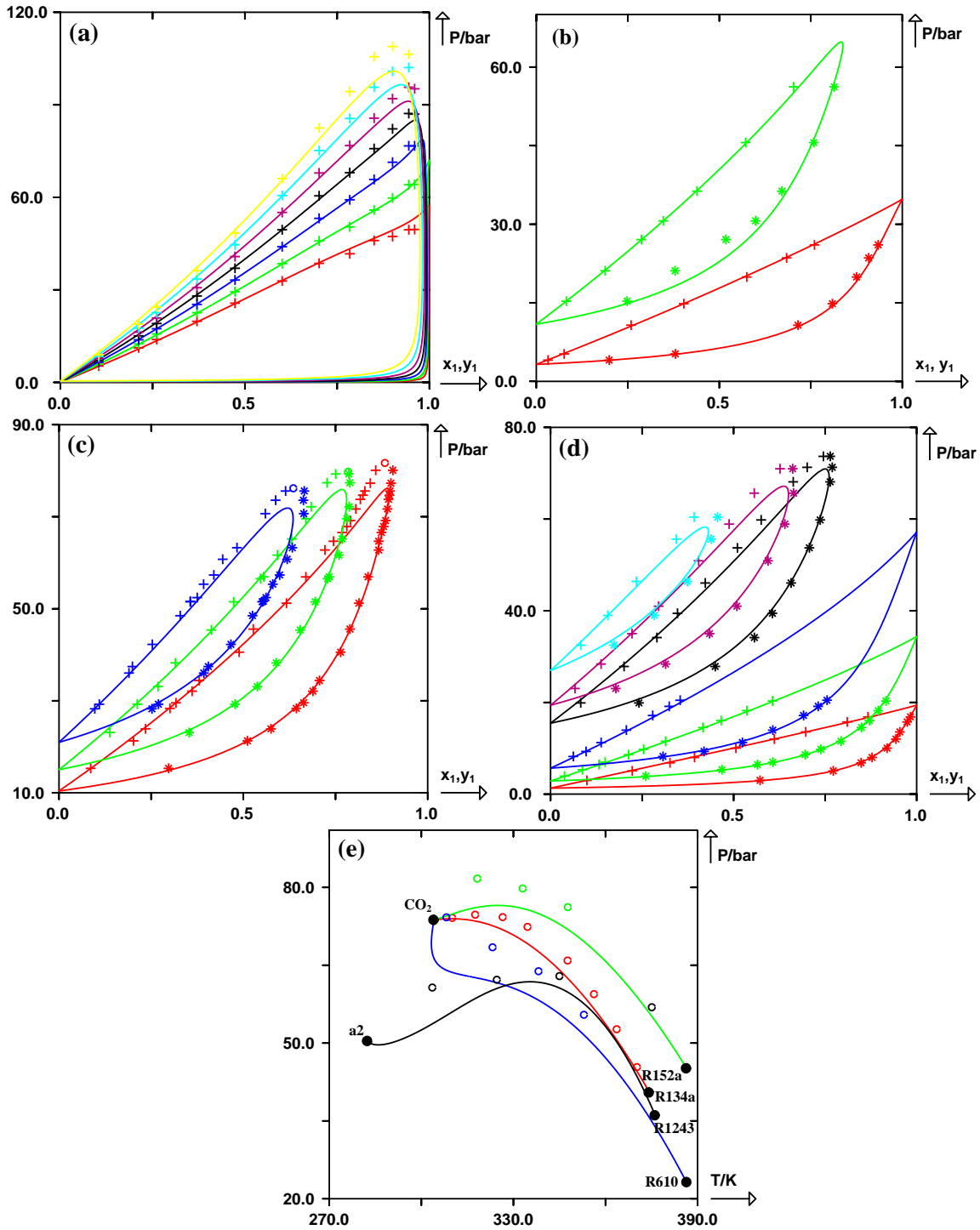


FIGURE 10

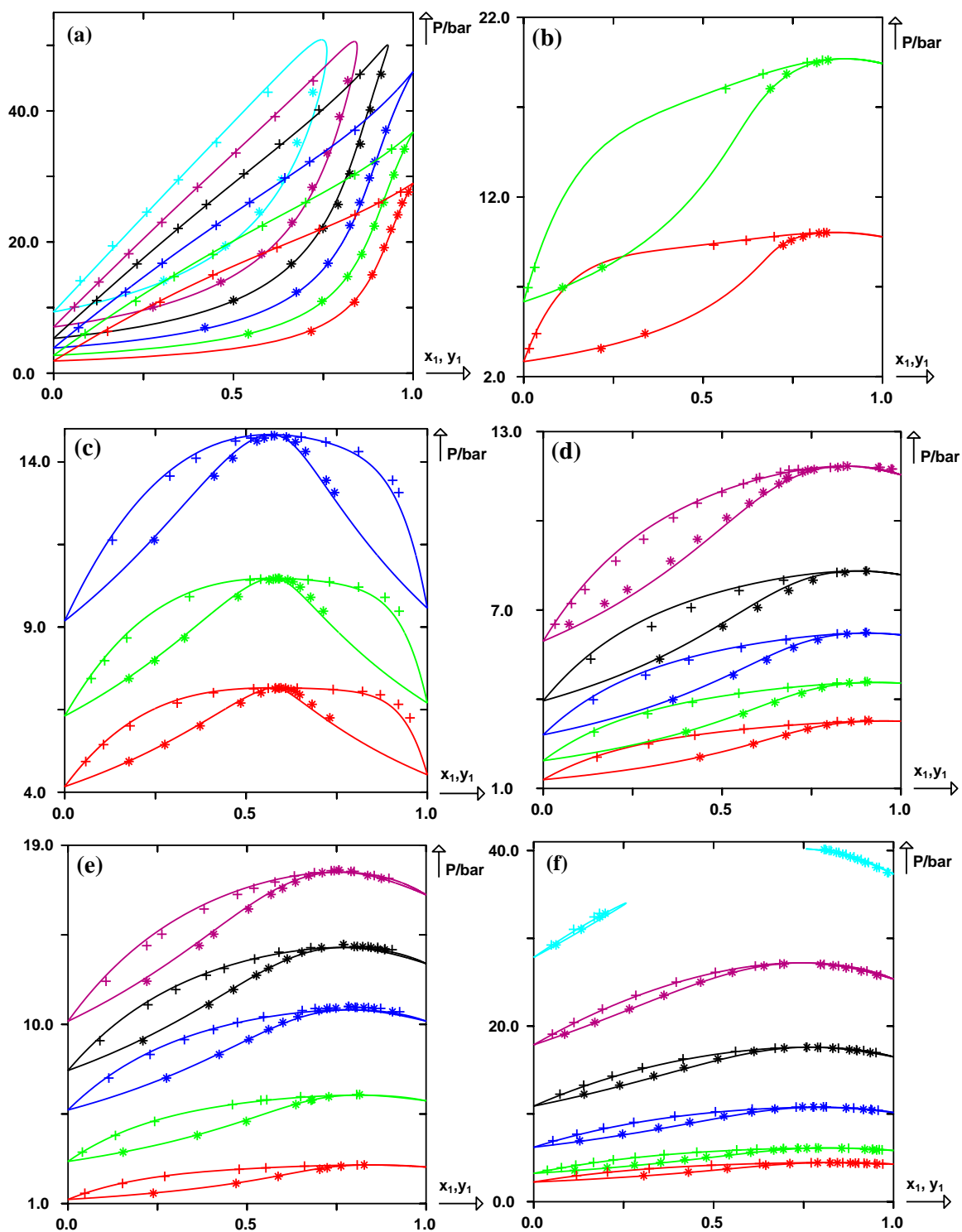
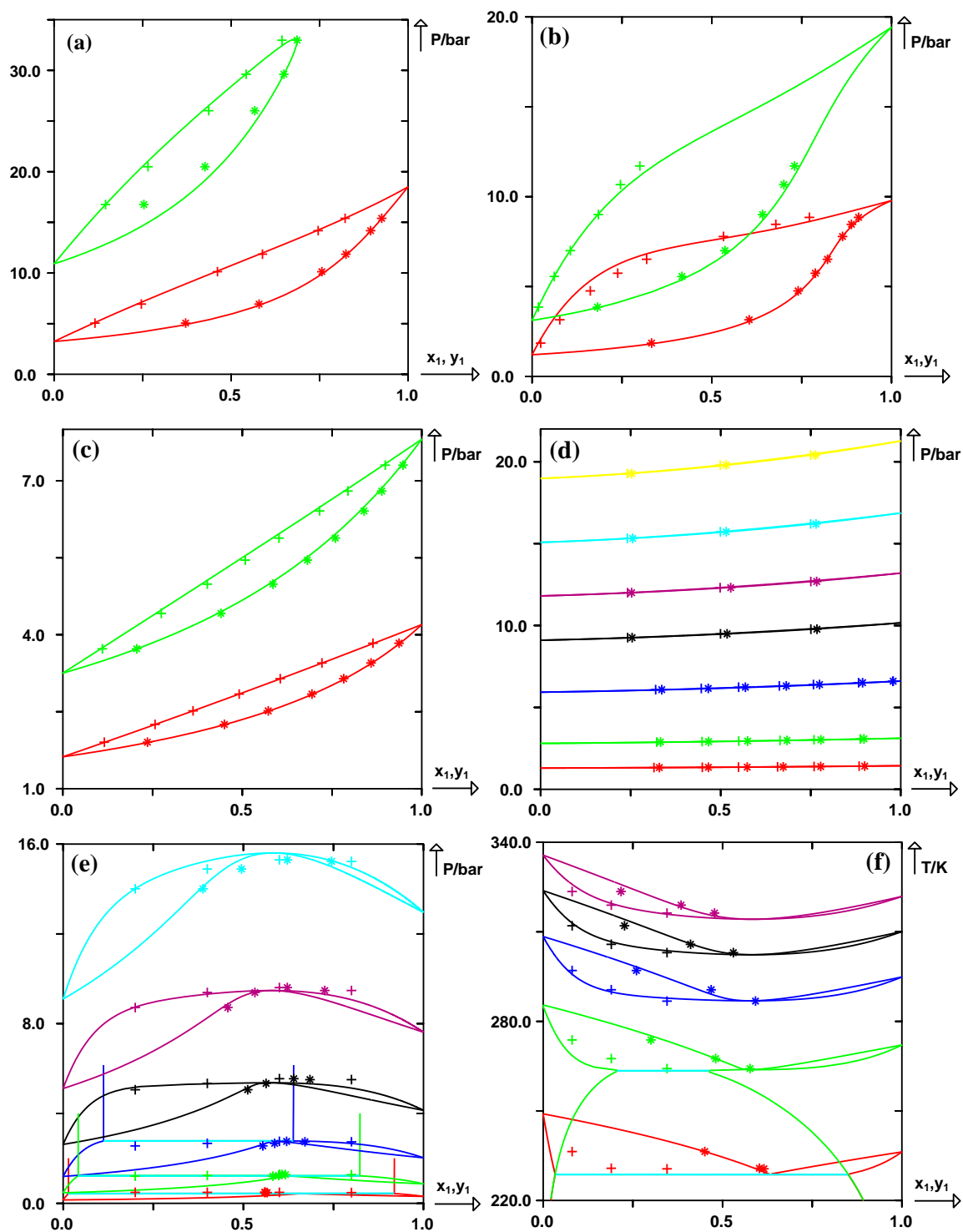


FIGURE 11



REFERENCES

- [1] C. Coquelet, A. Chareton, A. Valtz, A. Baba-Ahmed, D. Richon, Vapor-Liquid Equilibrium Data for the Azeotropic Difluoromethane + Propane System at Temperatures from 294.83 to 343.26 K and Pressures up to 5.4 MPa, *J. Chem. Eng. Data* 48 (2003) 317-323.
- [2] S.C. Subramoney, W.M. Nelson, A. Valtz, C. Coquelet, D. Richon, P. Naidoo, D. Ramjugernath, Pure Component and Binary Vapor-Liquid Equilibrium + Modeling for Hexafluoropropylene and Hexafluoropropylene Oxide with Toluene and Hexafluoroethane, *J. Chem. Eng. Data* 55 (2010) 411-418.
- [3] E. El Ahmar, A. Valtz, P. Naidoo, C. Coquelet, D. Ramjugernath, Isothermal Vapor-Liquid Equilibrium Data for the Perfluorobutane (R610) + Ethane System at Temperatures from (263 to 353) K, *J. Chem. Eng. Data* 56 (2011) 1918-1924.
- [4] A. Valtz, C. Coquelet, D. Richon, Vapor-liquid equilibrium data for the hexafluoroethane + carbon dioxide system at temperatures from 253 to 297 K and pressures up to 6.5MPa, *Fluid Phase Equilib.* 258 (2007) 179-185.
- [5] D. Ramjugernath, A. Valtz, C. Coquelet, D. Richon, Isothermal Vapor-Liquid Equilibrium Data for the Hexafluoroethane (R116) + Propane System at Temperatures from (263 to 323) K, *J. Chem. Eng. Data* 54 (2009) 1292-1296.
- [6] C. Coquelet, A. Valtz, P. Naidoo, D. Ramjugernath, D. Richon, Isothermal Vapor-Liquid Equilibrium Data for the Hexafluoropropylene (R1216) + Propylene System at Temperatures from (263.17 to 353.14) K, *J. Chem. Eng. Data* 55 (2010) 1636-1639.
- [7] W.M. Nelson, S.C. Subramoney, A. Valtz, C. Coquelet, D. Richon, P. Naidoo, D. Ramjugernath, Vapor-Liquid Equilibrium Data for Binary Systems Consisting of Either Hexafluoropropene (HFP) or 2,2,3-Trifluoro-3-(trifluoromethyl)oxirane (HFPO) with Carbon Dioxide (R-744) or 2,2-Dichloro-1,1,1-trifluoroethane (R-123), *J. Chem. Eng. Data* 56 (2011) 74-78.
- [8] A. Valtz, X. Courtial, E. Johansson, C. Coquelet, D. Ramjugernath, Isothermal vapor-liquid equilibrium data for the carbon dioxide (R744) + decafluorobutane (R610) system at temperatures from 263 to 353 K, *Fluid Phase Equilib.* 304 (2011) 44-51.
- [9] P. Morgado, C. McCabe, E.J.M. Filipe, Modelling the phase behaviour and excess properties of alkane + perfluoroalkane binary mixtures with the SAFT-VR approach, *Fluid Phase Equilib.* 228-229 (2005) 389-393.
- [10] M.J. Pratas de Melo, A.M.A. Dias, M. Blesic, L.P.N. Rebelo, L.F. Vega, J.A.P. Coutinho, I.M. Marrucho, Liquid-liquid equilibrium of (perfluoroalkane + alkane) binary mixtures, *Fluid Phase Equilib.* 242 (2006) 210-219.
- [11] S. Aparicio, Phase equilibria in perfluoroalkane+alkane binary systems from PC-SAFT equation of state, *J. Supercrit. Fluids* 46 (2008) 10-20.
- [12] R. Privat, J.N. Jaubert, Classification of global fluid-phase equilibrium behaviors in binary systems. *Chem. Eng. Res. Des.* 91 (2013) 1807-1839.
- [13] Y. Chen, F. Mutelet, J.N. Jaubert, Modeling the solubility of carbon dioxide in imidazolium based ionic liquids with the PC-SAFT equation of state. *J. Phys. Chem. B.* 116 (2012) 14375-14388.
- [14] T. Lafitte, A. Apostolakou, C. Avendaño, A. Galindo, C.S. Adjiman, E.A. Müller, G. Jackson, Accurate statistical associating fluid theory for chain molecules formed from Mie segments, *J. Chem. Phys.*, 139 (2013) 154504.
- [15] J.N. Jaubert, F. Mutelet, VLE predictions with the Peng-Robinson equation of state and temperature dependent k_{ij} calculated through a group contribution method, *Fluid Phase Equilib.* 224 (2004) 285-304.

- [16] J.N. Jaubert, S. Vitu, F. Mutelet, J.-P. Corriou, Extension of the PPR78 model (predictive 1978, Peng-Robinson EOS with temperature dependent k_{ij} calculated through a group contribution method) to systems containing aromatic compounds, *Fluid Phase Equilib.* 237 (2005) 193-211.
- [17] S. Vitu, J.N. Jaubert, F. Mutelet, Extension of the PPR78 model (Predictive 1978, Peng-Robinson EOS with temperature dependent k_{ij} calculated through a group contribution method) to systems containing naphthenic compounds, *Fluid Phase Equilib.* 243 (2006) 9-28.
- [18] J.-W. Qian, J.N. Jaubert, R. Privat, Prediction of the phase behavior of alkene-containing binary systems with the PPR78 model, *Fluid Phase Equilib.* 354 (2013) 212-235.
- [19] R. Privat, J.N. Jaubert, F. Mutelet, Addition of the Nitrogen Group to the PPR78 Model (Predictive 1978, Peng Robinson EOS with Temperature-Dependent k_{ij} Calculated through a Group Contribution Method), *Ind. Eng. Chem. Res.* 47 (2008) 2033-2048.
- [20] R. Privat, J.N. Jaubert, F. Mutelet, Use of the PPR78 Model To Predict New Equilibrium Data of Binary Systems Involving Hydrocarbons and Nitrogen. Comparison with Other GCEOS, *Ind. Eng. Chem. Res.* 47 (2008) 7483-7489.
- [21] S. Vitu, R. Privat, J.N. Jaubert, F. Mutelet, Predicting the phase equilibria of CO₂ + hydrocarbon systems with the PPR78 model (PR EOS and k_{ij} calculated through a group contribution method), *J. Supercrit. Fluids* 45 (2008) 1-26.
- [22] F. Mutelet, S. Vitu, R. Privat, J.N. Jaubert, Solubility of CO₂ in branched alkanes in order to extend the PPR78 model (Predictive 1978, Peng Robinson EoS with temperature-dependent k_{ij} calculated through a group contribution method) to such systems. *Fluid Phase Equilib.* 238 (2005) 157-168.
- [23] J.-W. Qian, J.N. Jaubert, R. Privat, Phase equilibria in hydrogen-containing binary systems modeled with the Peng-Robinson equation of state and temperature-dependent binary interaction parameters calculated through a group-contribution method, *J. Supercrit. Fluids* 75 (2013) 58-71.
- [24] V. Plee, J.N. Jaubert, R. Privat, P. Arpentinier, Extension of the E-PPR78 equation of state to predict fluid phase equilibria of natural gases containing carbon monoxide, helium-4 and argon, *J. Pet. Sci. Eng.* 133 (2015) 744-770.
- [25] X. Xu, R. Privat, J.N. Jaubert, Addition of the Sulfur Dioxide Group (SO₂), the Oxygen Group (O₂), and the Nitric Oxide Group (NO) to the E-PPR78 Model, *Ind. Eng. Chem. Res.* 54 (2015) 9494-9504.
- [26] R. Privat, J.N. Jaubert, F. Mutelet, Addition of the sulfhydryl group (-SH) to the PPR78 model (predictive 1978, Peng-Robinson EOS with temperature dependent k_{ij} calculated through a group contribution method), *J. Chem. Thermodyn.* 40 (2008) 1331-1341.
- [27] R. Privat, F. Mutelet, J.N. Jaubert, Addition of the Hydrogen Sulfide Group to the PPR78 Model (Predictive 1978, Peng-Robinson Equation of State with Temperature Dependent k_{ij} Calculated through a Group Contribution Method), *Ind. Eng. Chem. Res.* 47 (2008) 10041-10052.
- [28] R. Privat, J.N. Jaubert, Addition of the sulfhydryl group (SH) to the PPR78 model: Estimation of missing group-interaction parameters for systems containing mercaptans and carbon dioxide or nitrogen or methane, from newly published data, *Fluid Phase Equilib.* 334 (2012) 197-203.
- [29] J.-W. Qian, R. Privat, J.N. Jaubert, Predicting the Phase Equilibria, Critical Phenomena, and Mixing Enthalpies of Binary Aqueous Systems Containing Alkanes, Cycloalkanes, Aromatics, Alkenes, and Gases (N₂, CO₂, H₂S, H₂) with the PPR78 Equation of State, *Ind. Eng. Chem. Res.* 52 (2013) 16457-16490.
- [30] N. Juntarachat, R. Privat, L. Coniglio, J.N. Jaubert, Development of a Predictive Equation of State for CO₂ + Ethyl Ester Mixtures Based on Critical Points Measurements, *J. Chem. Eng. Data* 59 (2014) 3205-3219.

- [31] J.N. Jaubert, L. Coniglio, F. Denet, From the correlation of binary systems involving supercritical CO₂ and fatty acid esters to the prediction of (CO₂–fish oils) phase behavior. *Ind. Eng. Chem. Res.* 38 (1999) 3162–3171.
- [32] J.N. Jaubert, L. Coniglio, The group contribution concept: a useful tool to correlate binary systems and to predict the phase behavior of multicomponent systems involving supercritical CO₂ and fatty acids. *Ind. Eng. Chem. Res.* 38 (1999) 5011–5018.
- [33] N. Juntarachat, A. Valtz, C. Coquelet, R. Privat, J.N. Jaubert, Experimental measurements and correlation of vapor-liquid equilibrium and critical data for the CO₂ + R1234yf and CO₂ + R1234ze(E) binary mixtures. *Int. J. Refrigeration* 47 (2014) 141–152.
- [34] J.N. Jaubert, R. Privat, F. Mutelet, Predicting the phase equilibria of synthetic petroleum fluids with the PPR78 approach, *AIChE J.* 56 (2010) 3225–3235.
- [35] X. Xu, J.N. Jaubert, R. Privat, P. Duchet-Suchaux, F. Brana-Mulero, Predicting Binary-Interaction Parameters of Cubic Equations of State for Petroleum Fluids Containing Pseudo-components, *Ind. Eng. Chem. Res.* 54 (2015) 2816–2824.
- [36] J.N. Jaubert, L. Avaullée, C. Pierre, Is it still necessary to measure the minimum miscibility pressure? *Ind. Eng. Chem. Res.* 41 (2002) 303–310.
- [37] J.-W. Qian, R. Privat, J.N. Jaubert, P. Duchet-Suchaux, Enthalpy and heat capacity changes on mixing: fundamental aspects and prediction by means of the PPR78 cubic equation of state, *Energy Fuels* 27 (2013) 7150–7178.
- [38] J.-W. Qian, Développement du modèle E-PPR78 pour prédire les équilibres de phases et les grandeurs de mélange de systèmes complexes d'intérêt pétrolier sur de larges gammes de températures et de pressions, *Ph.D. thesis*, University of Lorraine, France (2011) 1–266.
- [39] J.N. Jaubert, R. Privat, Relationship between the binary interaction parameters (k_{ij}) of the Peng- Robinson and those of the Soave-Redlich-Kwong equations of state. Application to the definition of the PR2SRK model, *Fluid Phase Equilib.* 295 (2010) 26–37.
- [40] D.B. Robinson, D.Y. Peng, The characterization of the heptanes and heavier fractions for the GPA Peng-Robinson programs, *GPA Research Report* 28 (1978) 1–36.
- [41] B.E. Poling, J.M. Prausnitz, J.P. O'Connell, *The Properties of Gases and Liquids*, 5th Ed. (2000) 11–18.
- [42] J. Aftienjew, A. Zawisza, High-pressure liquid-vapour equilibria, critical state, and $p(V, T, x)$ up to 501.15 K and 4.560 MPa for n-pentane + n-perfluoropentane, *J. Chem. Thermodyn.* 9 (1977) 153–165.
- [43] M.V. Alekseeva, N.A. Smirnova, N.N. Sokolovskaya, Phase equilibria in systems containing perfluoroalkane. Communication II. Liquid-liquid-vapor equilibrium in ternary systems of alkanol-alkane-perfluoroalkane, *Zh. Prikl. Khim. (Leningrad)* 58 (1985) 1336–1340.
- [44] B. Bian, Measurement of Phase Equilibria in the Critical Region and Study of Equation of State, *Ph.D. thesis*, University of Nanjing, China (1992) 1–68.
- [45] S. Bobbo, R. Camporese, R. Stryjek, (Vapour + liquid) equilibrium measurement and correlation of the refrigerant (propane + 1,1,1,3,3,3-hexafluoropropane) at $T = (283.13, 303.19, \text{ and } 323.26) \text{ K}$, *J. Chem. Thermodyn.* 32 (2000) 1647–1656.
- [46] S. Bobbo, R. Stryjek, N. Elvassore, A. Bertucco, A recirculation apparatus for vapor-liquid equilibrium measurements of refrigerants. Binary mixtures of R600a, R134a and R236fa, *Fluid Phase Equilib.* 150, 151 (1998) 343–352.
- [47] G. Di Nicola, F. Polonara, R. Ricci, R. Stryjek, PVTx Measurements for the R116 + CO₂ and R41 + CO₂ Systems. New Isochoric Apparatus, *J. Chem. Eng. Data* 50 (2005) 312–318.
- [48] G. Di Nicola, F. Polonara, R. Stryjek, P-V-T-x and Vapor-Liquid Equilibrium Properties of Pentafluoroethane (R125) + 1,1,1,3,3,3-Hexafluoroethane [sic] (R236fa) and 1,1,1,2-Tetrafluoroethane (R134a) + R236fa Systems Derived from Isochoric Measurements, *J. Chem. Eng. Data* 46 (2001) 359–366.

- [49] A.M.A. Dias, H. Carrier, J.L. Daridon, J.C. Pamies, L.F. Vega, J.A.P. Coutinho, I.M. Marrucho, Vapor-Liquid Equilibrium of Carbon Dioxide-Perfluoroalkane Mixtures: Experimental Data and SAFT Modeling, *Ind. Eng. Chem. Res.* 45 (2006) 2341-2350.
- [50] A. Didier, J.C. Tanguy, D. Sallet, European Patent (1990).
- [51] R.D. Dunlap, R.G. Bedford, J.C. Woodbrey, S.D. Furrow, Liquid-vapor equilibrium for the system: perfluoro-n-hexane-n-hexane, *J. Am. Chem. Soc.* 81 (1959) 2927-2930.
- [52] C. Duran-Valencia, G. Pointurier, A. Valtz, P. Guilbot, D. Richon, Vapor-Liquid Equilibrium (VLE) Data for the Carbon Dioxide (CO₂) + 1,1,1,2-Tetrafluoroethane (R134a) System at Temperatures from 252.95 K to 292.95 K and Pressures up to 2 MPa, *J. Chem. Eng. Data* 47 (2002) 59-61.
- [53] F.D. Evans, R. Battino, Solubility of gases in liquids. 3. Solubilities of gases in hexafluorobenzene and in benzene, *J. Chem. Thermodyn.* 3 (1971) 753-760.
- [54] E. Fransson, A. Barreau, J. Vidal, Vapor-liquid equilibrium in binary systems of n-pentane + chlorodifluoromethane or + 1,1-difluoroethane, *J. Chem. Eng. Data* 37 (1992) 521-525.
- [55] J.B. Gilmour, J.O. Zwicker, J. Katz, R.L. Scott, Fluorocarbon solutions at low temperatures. V. The liquid mixtures C₂H₆ + C₂F₆, C₃H₈ + C₂F₆, CH₄ + C₃F₈, C₂H₆ + C₃F₈, C₃H₈ + C₃F₈, C₄C₁₀ + C₃F₈, iso-C₄H₁₀ + C₃F₈, C₃H₈ + C₄F₁₀, n-C₆H₁₄ + C₄F₁₀, n-C₇H₁₆ + C₄F₁₀, n-C₉H₂₀ + n-C₄F₁₀, and n-C₁₀H₂₂ + n-C₄F₁₀, *J. Phys. Chem.* 71 (1967) 3259-3270.
- [56] Q.N. Ho, B.G. Lee, J.-Y. Park, J.-D. Kim, J.S. Lim, Measurement of vapor-liquid equilibria for the binary mixture of propylene (R-1270) + 1,1,1,2-tetrafluoroethane (HFC-134a), *Fluid Phase Equilib.* 225 (2004) 125-132.
- [57] C.D. Holcomb, J.W. Magee, J.L. Scott, S.L. Outcalt, W.M. Haynes, NIST Technical Note 1397 - Selected Thermodynamic Properties for Mixtures of R-32 (Difluoromethane), R-125 (Pentafluoroethane), R-134A (1,1,1,2-Tetrafluoroethane), R-143A (1,1,1-Trifluoroethane), R-41 (Fluoromethane), R-290 (Propane), and R744 (Carbon Dioxide), Report (1997) A1-A87.
- [58] J. Im, M. Kim, B.-G. Lee, H. Kim, Vapor-Liquid Equilibria of the Binary n-Butane (HC-600) + Difluoromethane (HFC-32), + Pentafluoroethane (HFC-125), + 1,1,1,2-Tetrafluoroethane (HFC-134a) Systems, *J. Chem. Eng. Data* 50 (2005) 359-363.
- [59] R. Jadot, M. Fraiha, Isobaric vapor-liquid equilibrium of (trifluoromethyl)benzene with benzene, toluene, or chlorobenzene, *J. Chem. Eng. Data* 37 (1992) 509-511.
- [60] R. Jadot, M. Frere, Simulation of liquid-vapor equilibria of hydrofluorocarbon (HFC) mixtures by the UNIFAC model, *High Temp. - High Pressures* 25 (1993) 491-501.
- [61] L.W. Jordan, Jr., W.B. Kay, Phase relations of binary systems that form azeotropes-n-alkanes-perfluoro-n-heptane systems (ethane through n-nonane), *Chem. Eng. Prog., Symp. Ser.* 59 (1963) 46-51.
- [62] Y.W. Kho, D.C. Conrad, B.L. Knutson, Phase equilibria and thermophysical properties of carbon dioxide-expanded fluorinated solvents, *Fluid Phase Equilib.* 206 (2003) 179-193.
- [63] M. Kleiber, Vapor-liquid equilibria of binary refrigerant mixtures containing propylene or R134a, *Fluid Phase Equilib.* 92 (1994) 149-194.
- [64] Y. Kobatake, J.H. Hildebrand, Solubility and entropy of solution of He, N₂, Ar, O₂, CH₄, C₂H₆, CO₂, and SF₆ in various solvents; regularity of gas solubilities, *J. Phys. Chem.* 65 (1961) 331-335.
- [65] A. Kordikowski, D.G. Robertson, A.I. Aguiar-Ricardo, V.K. Popov, S.M. Howdle, M. Poliakov, Probing Vapor/Liquid Equilibria of Near-Critical Binary Gas Mixtures by Acoustic Measurements, *J. Phys. Chem.* 100 (1996) 9522-9526.
- [66] S. Kramp, A. Sander, H.G. Wagner, The Vapor-Liquid Equilibria of Binary Systems Consisting of Fluorinated Hydrocarbons and Hydrocarbons, *Chem. Ing. Tech.* 61 (1989) 664-665.

- [67] A.P. Kuznetsov, I.V. Volobuev, V.I. Los, M.G. Khmel'nyuk, Study of phase equilibrium of a mixture of R152A-R218 refrigerants, *Kholodil'n. Tekhn. i Tekhnol.*, Kiev (1982) 93-96.
- [68] M.J. Lazzaroni, D. Bush, J.S. Brown, C.A. Eckert, High-pressure vapor-liquid equilibria of some carbon dioxide + organic binary systems, *J. Chem. Eng. Data* 50 (2005) 60-65.
- [69] J.S. Lim, J.-Y. Park, J.W. Kang, B.-G. Lee, Measurement of vapor-liquid equilibria for the binary systems of propane + 1,1,1,2-tetrafluoroethane and 1,1,1-trifluoroethane + propane at various temperatures, *Fluid Phase Equilib.* 243 (2006) 57-63.
- [70] J.S. Lim, J.-Y. Park, B.-G. Lee, Y.-W. Lee, J.-D. Kim, Phase equilibria of CFC alternative refrigerant mixtures. Binary systems of isobutane + 1,1,1,2-tetrafluoroethane, + 1,1-difluoroethane, and + difluoromethane, *J. Chem. Eng. Data* 44 (1999) 1226-1230.
- [71] J.W. Mausteller, The Departure of n-Butforane and n-Butane Solutions from Ideality, *Ph.D. thesis*, Pennsylvania (1951) 1-56.
- [72] K.W. Miller, Solubility of fluorocarbon gases in cyclohexane, *J. Phys. Chem.* 72 (1968) 2248-2249.
- [73] B. Minor, K. King, Azeotropic Compositions of Cyclopentane, US Patent. (1997) 1-21.
- [74] A.E.H.N. Mousa, W.B. Kay, A. Kreglewski, Critical constants of binary mixtures of certain perfluoro-compounds with alkanes, *J. Chem. Thermodyn.* 4 (1972) 301-311.
- [75] C.R. Mueller, J.E. Lewis, Thermodynamic and transport properties of the system iso.ovrddot.octane and perfluoroheptane, *J. Chem. Phys.* 26 (1957) 286-292.
- [76] J.A. Neff, J.B. Hickman, Total pressure over certain binary liquid mixtures, *J. Phys. Chem.* 59 (1955) 42-45.
- [77] K. Ohgaki, M. Kageyama, T. Katayama, Pressure-volume-composition (p-Vml-x,y) relations for azeotropic mixture of 1,1-difluoroethane and propylene, *J. Chem. Eng. Jpn.* 23 (1990) 763-764.
- [78] Y. Shi, K. Wang, H. Liu, Y. Hu, Measurement of vapor-liquid equilibria for 1,1,1,2-tetrafluoroethane-1,1-difluoroethane binary system, *Huadong Ligong Daxue Xuebao* 21 (1995) 613-618.
- [79] M.B. Shiflett, B. Minor, US Patent. (1994) 1-18.
- [80] M.B. Shiflett, S.I. Sandler, Modeling fluorocarbon vapor-liquid equilibria using the Wong-Sandler model, *Fluid Phase Equilib.* 147 (1998) 145-162.
- [81] G. Silva-Oliver, L.A. Galicia-Luna, Vapor-liquid equilibria for carbon dioxide + 1,1,1,2-tetrafluoroethane (R-134a) systems at temperatures from 329 to 354 K and pressures up to 7.37 MPa, *Fluid Phase Equilib.* 199 (2002) 213-222.
- [82] J.H. Simons, R.D. Dunlap, The properties of n-pentforane [perfluoropentane] and its mixtures with n-pentane, *J. Chem. Phys.* 18 (1950) 335-346.
- [83] J. Storm, Application of the UNIFAC-method for the prediction of vaporization equilibria of refrigerant mixtures, Dissertation (TU Braunschweig) (1989).
- [84] R. Stryjek, S. Bobbo, R. Camporese, Isothermal Vapor-Liquid Equilibria for 1,1,1,2-Tetrafluoroethane + Propane and Propane + 1,1,1-Trifluoroethane at 283.18 K, *J. Chem. Eng. Data* 43 (1998) 241-244.
- [85] R. Tillner-Roth, An experimental study of the thermodynamic properties of the refrigerant mixture: {1,1,1,2-tetrafluoroethane (R 134a) + 1,1-difluoroethane (R 152a)}, *J. Chem. Thermodyn.* 25 (1993) 1419-1441.
- [86] I.V. Volobuev, M.G. Khmel'nyuk, P.S. Bolkhovskii, Thermodynamic properties of a R-152A-R-218 mixture, *Kholod. Tekhn. i Tekhnol.*, Kiev (1984) 68-71.
- [87] X. Yang, Contribution to the experimental Investigation and Calculation of Vapor-Liquid Phase Equilibria, Dissertation (TU Berlin) (1991) 1-189.
- [88] V.S. Zernov, V.B. Kogan, S.G. Lyubetskii, F.I. Duntov, Liquid-vapor equilibrium in the ethylene-trifluoropropylene system, *Zh. Prikl. Khim. (Leningrad)* 44 (1971) 683-686.

- [89] Y. Zhang, M. Gong, H. Zhu, J. Wu, Vapor-Liquid Equilibrium Measurements for the Ethane + Hexafluoroethane System over a Temperature Range from (199.64 to 242.93) K, *J. Chem. Eng. Data* 50 (2005) 2074-2076.
- [90] Y. Zhang, M.-Q. Gong, H.-B. Zhu, J.-F. Wu, Vapor-liquid equilibrium measurements and correlations for an azeotropic system of ethane + hexafluoroethane, *Fluid Phase Equilib.* 240 (2006) 73-78.
- [91] S.C. Subramoney, P. Naidoo, A. Valtz, C. Coquelet, D. Richon, D. Ramjugernath, Experimental vapor + liquid equilibrium data and modelling for binary mixtures of decafluorobutane with propane and 1-butene, *J. Chem. Thermodyn.* 67 (2013) 134-142.
- [92] E. El Ahmar, A. Valtz, P. Paricaud, C. Coquelet, L. Abbas, W. Rached, Vapor-liquid equilibrium of binary systems containing pentafluorochemicals from 363 to 413 K: Measurement and modelling with Peng-Robinson and three SAFT-like equations of states. *Int. J. Refrigeration* 35 (2012) 2297-2310.
- [93] S.C. Subramoney, A. Valtz, C. Coquelet, D. Richon, P. Naidoo, D. Ramjugernath, Vapor-liquid equilibrium measurements and modeling for the ethane (R-170) + 1,1,2,3,3,3-hexafluoro-1-propene (R-1216) binary system. *J. Chem. Eng. Data* 57 (2012) 2947-2955.
- [94] S.C. Subramoney, X. Courtial, P. Naidoo, C. Coquelet, D. Richon, D. Ramjugernath, Isothermal vapor-liquid equilibrium data for the ethylene + 1,1,2,3,3,3-hexafluoro-1-propene binary system between 258 and 308 K at pressures up to 4.56 MPa. *Fluid Phase Equilib.* 353 (2013) 7-14.
- [95] C. Coquelet, D. Ramjugernath, H. Madani, A. Valtz, P. Naidoo, A.H. Meniai, Experimental Measurement of Volumetric Properties and Modelling of Critical Properties for Pure Hexafluoropropylene, *J. Chem. Eng. Data* 55 (2010) 2093-2099.
- [96] C. Coquelet, D. Richon, Experimental Determination of Phase Diagram and Modeling. Application to Refrigerant Mixtures, *Int. J. Refrigeration* 32 (2009) 1604-1614.
- [97] P.H. Van Konynenburg, R.L. Scott, Critical lines and phase equilibria in binary van der Waals mixtures, *Philos. Trans. R. Soc. London, Ser. A* 298 (1980) 495-540.
- [98] J.N. Jaubert, R. Privat, Possible existence of a negative (positive) homogeneous azeotrope when the binary mixture exhibits positive (negative) deviations from ideal solution behavior (that is when g^E is positive (negative)), *Ind. Eng. Chem. Res.* 45 (2006) 8217-8222.
- [99] J.N. Jaubert, R. Privat, N. Juntarachat, General reflection on critical negative azeotropy and upgrade of the Bancroft's rule with application to the Acetone + Chloroform binary system. *J. Supercrit. Fluids.* 94 (2014) 17-29.